

Mass spectrometry of organic matter influenced by long-term pedogenesis and a short-term reclamation practice in an Oxisol of Brazil

Carlos M. Monreal, Marlene Cristina Alves, Morris Schnitzer, Sebastiao Nilce Souto Filho, and Carolina dos Santos Batista Bonini

Abstract: Little is known about the influence of soil pedogenesis and reclamation practices on the chemical composition of soil organic matter (SOM) in eroded Oxisol. We examined the long-term influence of pedogenesis and 8 years of a reclamation practice on SOM in the top 5 cm of an artificially eroded Oxisol of Brazil. The experimental site involved replicated treatments established under native vegetation, and an adjacent site whose top 8.6 m had been removed mechanically (eroded reference). The eroded Oxisol was under reclamation with native tree and grass species, and addition of sewage sludge. Pyrolysis field ionization mass spectrometry was used to characterize SOM. The abundance of most classes of SOM and soil carbon decreased in the following order: native > reclaimed >> eroded soil. Relative to the eroded reference, SOM in the native soil was highly humified and stabilized by inorganic colloids of iron, aluminum, and silicon. Humified and thermally stable SOM in the native and reference eroded soils involved mostly alkylaromatics, lipids, phenols+lignin monomers, lignin dimers, and N-heterocyclics. The reclaimed soil SOM was less humified and less stable than the native Oxisol, showing significant contributions of carbohydrates, amino acids, and sterols derived from sewage sludge and plant residues.

Key words: oxisol, soil organic matter, chemical classes, mass spectrometry, erosion, soil reclamation.

Résumé : On sait peu de choses concernant l'influence de la pédogenèse et des pratiques de restauration du sol sur la composition chimique de la matière organique dans les oxisols érodés. Les auteurs ont étudié les effets à long terme de la pédogenèse et de 8 années de restauration du sol sur la matière organique présente dans la couche supérieure de 5 cm d'un oxisol du Brésil érodé artificiellement. Le site expérimental a fait l'objet de traitements répétés sous la végétation indigène, tandis qu'on a retiré mécaniquement la couche supérieure de 8,6 m d'un site adjacent afin d'en faire un site témoin sur le plan de l'érosion. L'oxisol érodé avait subi des travaux de restauration sous forme de plantation d'espèces indigènes d'arbres et de graminées, après enrichissement avec des boues usées. Les chercheurs ont recouru à un spectromètre de masse à ionisation portatif avec pyrolyse pour caractériser la matière organique. L'abondance de la plupart des classes de matière organique et de carbone organique diminue dans l'ordre suivant : sol intact > sol restauré >> sol érodé. Lorsqu'on effectue une comparaison avec le témoin érodé, on constate que la matière organique du sol naturel est très humifiée et que des colloïdes du fer, de l'aluminium et du silicium la stabilisent. La matière organique humifiée et thermiquement stable du sol naturel et du sol érodé utilisé comme témoin renferme surtout des alkylaromatiques, des lipides, des phénols combinés à des monomères de la lignine, des dimères de la lignine et des N-hétérocycliques. Celle du sol restauré est moins humifiée et moins stable que celle de l'oxisol naturel, avec d'importants apports d'hydrates de carbone, d'acides aminés et de stérols ayant pour origine les boues usées et des résidus végétaux. [Traduit par la Rédaction].

Mots-clés : oxisol, matière organique du sol, classes chimiques, spectrométrie de masse, érosion, restauration du sol.

Introduction

Soil organic matter (SOM) is central to sustaining and enhancing the quality and productivity of cultivated

land (Monreal et al. 1995). Organic matter (OM) influences water retention, soil fertility, and structural stability, and as such, SOM is often used as an indicator of soil

Received 11 March 2015. Accepted 25 September 2015.

C.M. Monreal and M. Schnitzer. Eastern Cereal and Oilseed Research Centre, Agriculture and Agri-Food Canada, Ottawa, Ontario, Canada.

M.C. Alves, S.N.S. Filho, and C.S. Batista Bonini. Departamento de Fitossanidade Engenharia Rural e Solos, Universidade Estadual Paulista, São Paulo, Brazil.

Corresponding author: Carlos M. Monreal (email: carlos.monreal@agr.gc.ca).

quality and for the successful management of savannas (Feigl et al. 1995; Dexter 2004). Chemical components of SOM, such as lipids and polysaccharides, influence soil aggregate and structure stability; amino acids and N-heterocyclics may be used as substrates for the biotic mineralization of soil organic nitrogen (N). Compounds of SOM, such as alkaloids, fatty acids, alkylamides, and polyphenols in SOM, represent metabolites of chemical signalling networks reflecting specific ecological functions in crop rhizospheres (Monreal and Schnitzer 2013, 2015).

The change in land use from natural grasslands to cropped land greatly affects the structural stability and decreases OM content in Oxisols of Brazil (Zinn et al. 2005) and in Acrisols and Luvisols of Mexico and Mollisols of Canada (van Veen and Paul 1981; Monreal et al. 2005). Intense conversion of forest to agricultural land has been a frequent land use change in areas of Brazil and other countries (Fearnside 1993). In tropical areas, changes in land use shift the composition of vegetation, which in turn affects the amount and quality of SOM input and the diversity of soil macro- and microfauna and microbial communities (Lavelle and Pashanasi 1989; Johnson et al. 2003). In general, agroforestry enhances nutrient storage after land conversion as compared with sole cropping systems in semitropical and tropical regions (Isaac et al. 2005; Monreal et al. 2005). Determining the impact of human activities on SOM in the tropics is of interest owing to sustainability risks to food security associated with increased agricultural, deforestation, and urbanization activities (Hernández and López 2002), and these activities can be examined using simulation models (Wendling et al. 2014).

Building hydroelectric dams involves anthropogenic activities that remove native vegetation, soil profiles, and surficial geologic deposits and result in land flooding. These engineering activities may catalyze the beginning of ecosystem degradation. The loss of topsoil is central to landscape restoration. Although agricultural land use takes into account soil fertility in as much as it affects crop growth, topsoil is equally important for storing OM that supports biological diversity and activities essential for nutrient cycling and maintenance of soil health and natural conservation services. In general, anthropogenically eroded areas display low resilience such that they cannot return to their previous state or the return happens extremely slowly. When measures for recovery are not taken, soil degradation may continue for many years. Reclamation measures can focus on the landscape recovery and also on the maintenance of the productive potential of the affected zone (Taboada-Castro et al. 2009).

Little is known about the effects of man-made soil erosion and subsequent reclamation practices on the amounts and chemical quality of SOM in Oxisols of Brazil. The objective of this study was to determine the amount and chemical composition of SOM in an Oxisol

under native vegetation and in an adjacent eroded Oxisol that has been under reclamation for 8 years with plants and sewage sludge addition. An Oxisol whose top 8.6 m was mechanically removed for building a nearby hydro dam was used as a reference soil treatment to study changes in SOM chemical composition by pyrolysis field ionization mass spectrometry (Py-FIMS).

Materials and Methods

Field research plots were established to test the hypothesis that pedogenesis and reclamation practices influence the amount and distribution of chemical structures of SOM in an Oxisol of Brazil.

Field location and climate

The experimental research plots were established on flat land at the Experimental Farm of the Faculty of Engineering, Campus de Ilha Solteira of the Universidade Estadual Paulista, São Paulo, Brazil, in February 2004. The site is located 327 m above sea level and at 51°22'W, 20°22'S. The average annual rainfall is 1370 mm, the air temperature is 23.5 °C with a relative air humidity of 75%.

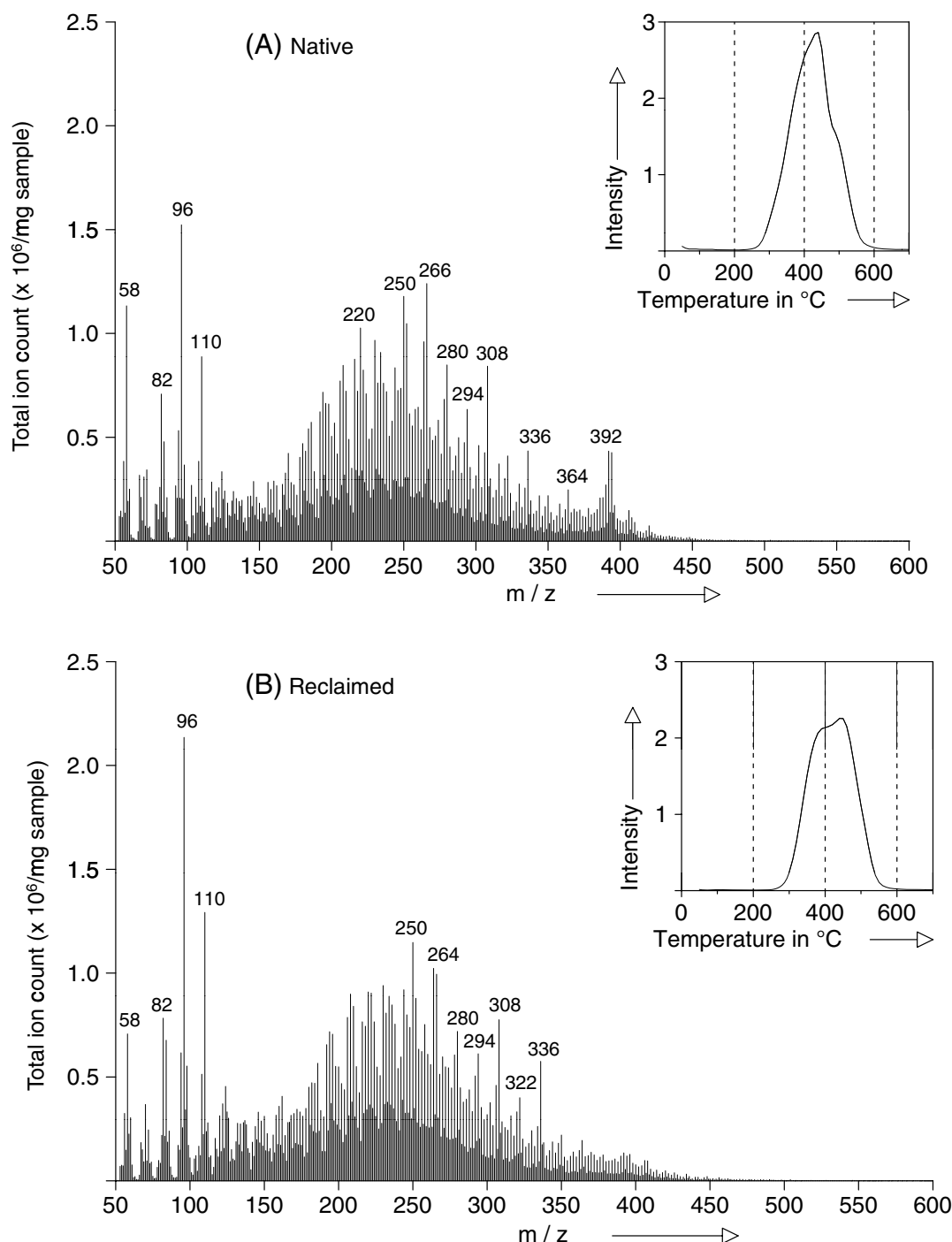
Soil and treatments

In 2004, field plots (12 m × 8 m) were established in a weathered Oxisol of sandy clay loam to sandy loam texture (EMBRAPA 2013). The field experiment was set as a completely randomized block, with three soil treatments; each treatment was replicated four times. Treatment 1 involved mechanically induced soil erosion of a native Savanna soil, where the top 8.6 m (including the A horizon and part of the B horizon) of soil was removed. Treatment 1, which had no plant cover, was used as a reference eroded benchmark soil to study the amount and chemical changes of OM in the other two treatments. Treatment 2 (native Oxisol) involved an undisturbed Oxisol site under various plant species described in the subsequent section. Treatment 3 (reclaimed Oxisol) involved the mechanically eroded soil planted with tree and grass species together with addition of sewage sludge and lime. The research plots for Treatments 1 and 3 that were established in the eroded Oxisol on saprolite, have a less weathered regolith than the original native Oxisol (Kitamura et al. 2008; Taboada-Castro et al. 2009).

Vegetation and reclamation practice

Under soil Treatment 2, the native Oxisol had a permanent cover of mixed trees, including *Curatella americana*, *Stryphnodendron adstringens*, *Byrsonima verbascifolia*, and *Astronium fraxinifolium* Schott. The last tree species are hardwood perennial species native to Brazil, belonging to the family Anacardiaceae. The soil plots undergoing the reclamation practice (Treatment 3) were planted with trees and grasses in year 1 of the study. The tree species was *Astronium fraxinifolium* Schott planted in a spacing of 3 m × 2 m to give a density of 25 trees plot⁻¹. The

Fig. 1. Py-FIMS spectra for soil organic matter found in the 0–5 cm depth of the (A) native Oxisol, (B) reclaimed Oxisol, and (C) reference eroded Oxisol.



grass *Urochloa decumbens* Stapf was seeded at a rate of 16 kg ha⁻¹ between the tree rows (3 m apart). The soil reclamation treatment also received a one-time addition of municipal sewage sludge (60 t ha⁻¹, dry basis) and a one-time addition of dolomite lime (CaO: 28–31% w/w; MgO: 18–21% w/w) applied at 2 t ha⁻¹ in February 2004. The sewage sludge and lime were incorporated and mixed into the soil with a plow to 20 cm depth, then harrowed and levelled. There was no vegetation growing in

the reference eroded soil Treatment 1. Further details on other tillage equipment and operations, spatial distribution of plots, and some chemical and physical properties of the studied soils have been published earlier by [Alves and Suzuki \(2007\)](#).

Soil sampling, sample processing and analysis

In 2012, soil samples were taken with a handheld core sampler (8 cm diameter) from the 0–5 cm soil depth, at

Fig. 1 (concluded).

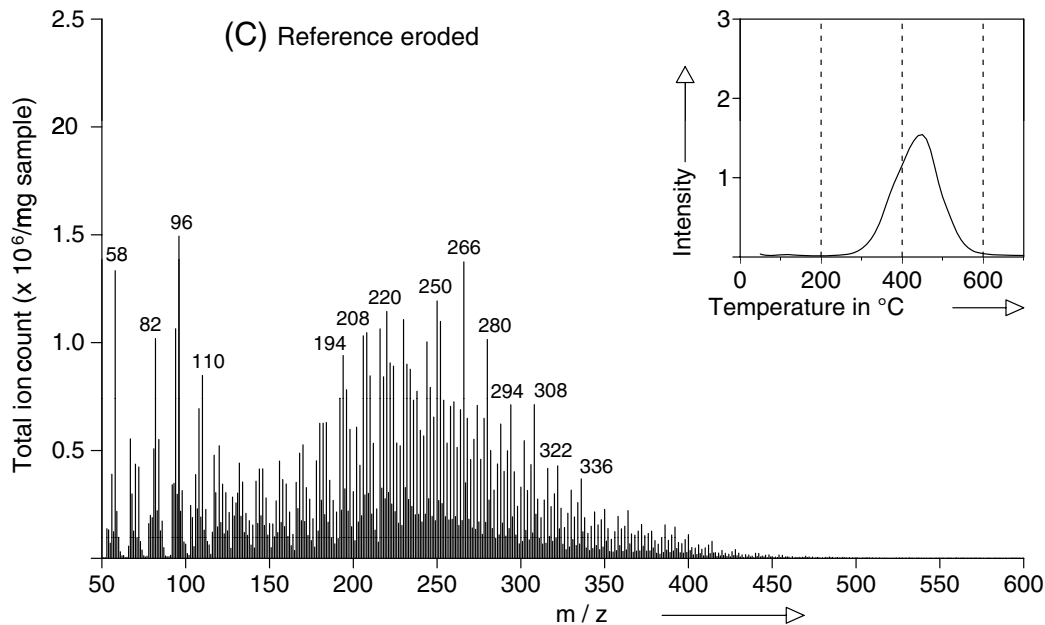


Table 1. The content of inorganic and organic components in the 0–5 cm depth of a native and reclaimed relative to a reference eroded Oxisol.

Treatment	Fe (mg g ⁻¹)	Fe ₂ O ₃ (%)	Al+H (mmol _c dm ⁻³)	SiO ₂ (%)	Total C		Total N		C/N*
					(mg kg ⁻¹)	(t ha ⁻¹)	(mg kg ⁻¹)	(t ha ⁻¹)	
Native	29.8a	6.3a	48.8a	75.4a	20.37a	10.80a	1.17a	0.62a	17.4
Reclaimed	30.0a	7.5a	21.0b	70.9a	8.50b	6.25b	0.55b	0.40b	15.5
Reference eroded	29.8a	6.9a	15.6c	71.3a	5.39b	4.21b	0.37b	0.29b	14.6
MSD [†]	5.80	1.30	5.03	5.00	4.87	3.88	0.24	0.15	
CV (%) [‡]	7.75	7.42	12.33	2.75	14.4	18.8	12.0	12.3	

Note: Within each column, values not followed by the same letter are significantly different at the 5% level (Tukey test).

*C/N value rounded up to the next digit.

[†]MSD, minimum significant difference ($p < 0.05$).

[‡]CV, coefficient of variation.

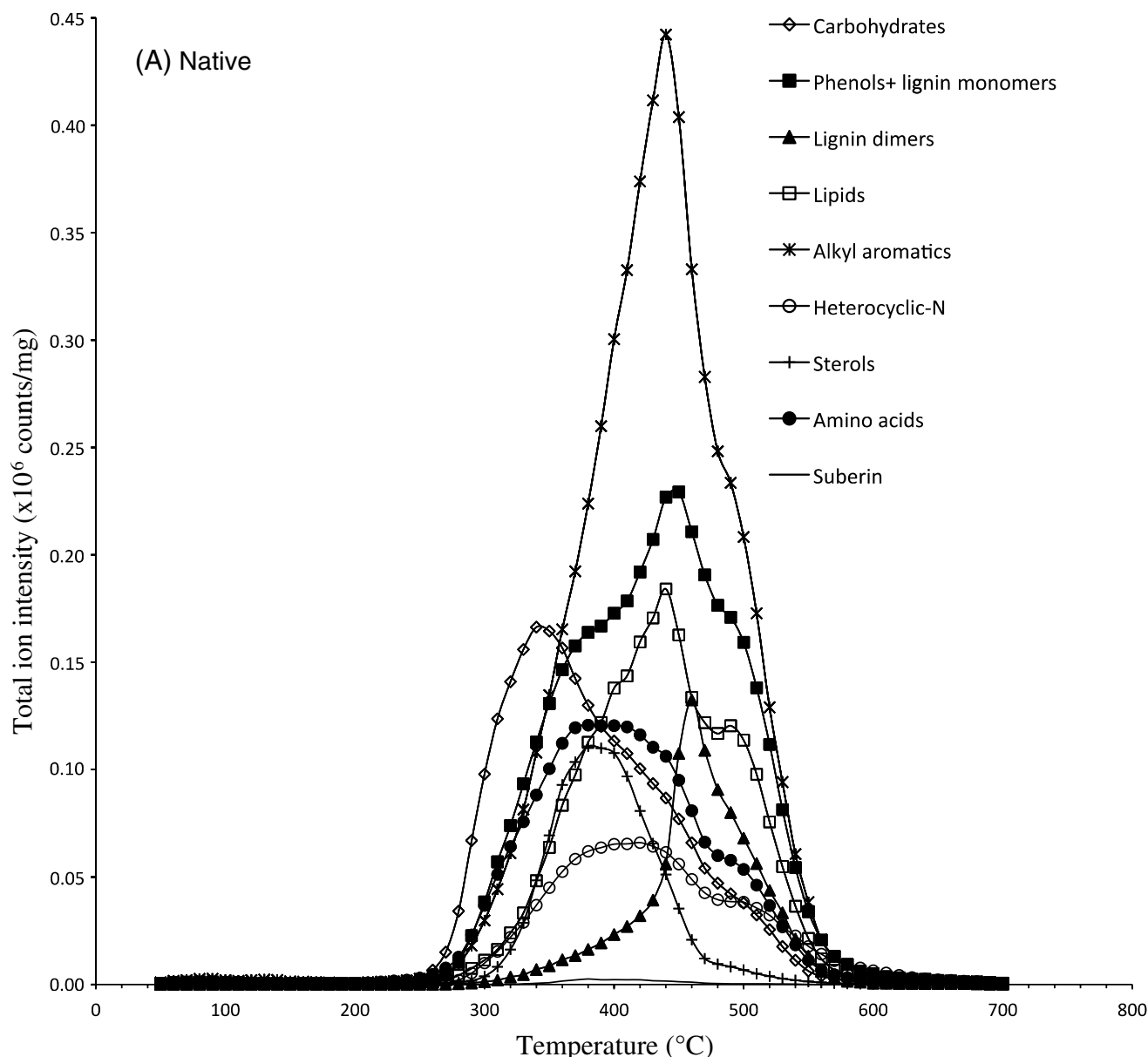
five randomly selected locations inside each replicated treatment plot. For example, soil samples from the surface 0–5 cm depth were collected from the A horizon in the native site, and from the 0–5 cm depth of the saprolite soil substrate in the reclaimed and reference eroded Oxisols. The five samples taken randomly from each replicated plot were pooled together into a composite sample and mixed thoroughly to produce a representative soil sample. Collected soil samples were oven-dried at 105 °C and ground to pass through a 100-mesh sieve before physical and chemical analysis.

Soil particle size analysis followed the pipette method (EMBRAPA 1997). Total iron (Fe), Fe₂O₃, and SiO₂ were analyzed by X-ray fluorescence spectrometry, and mineral components were microwave extracted with nitric acid and subsequently analyzed by inductively coupled plasma mass spectrometry (UH 2011). The content of

Al+H species (potential acidity) was determined by soil extraction with calcium chloride (0.01 mol L⁻¹) buffered with the Shoemaker, McLean, and Pratt solution at pH 7.5 (van Raij et al. 2001). The Al+H represents the aluminum (Al) species in the soil solution and easily exchangeable pools determined by titration. Other chemical and morphological properties of the soil and chemical composition of the sewage sludge have been reported by Paz-Ferreiro and Alves (2012) and Bonini et al. (2015).

The concentration (%w/w) of carbon (C) and N were determined by dry combustion at the stable isotope laboratory of the University of Ottawa. The soil samples were weighed into tin capsules and flash combusted with oxygen at 1800 °C and carried by helium through columns of reducing–oxidizing chemicals to get N₂ and CO₂. The gases were separated by “trap and purge”

Fig. 2. Thermograms of selected classes for organic compounds volatilized from the (A) native Oxisol, (B) reclaimed Oxisol, and (C) reference eroded Oxisol.



of specific adsorption columns so that the thermal conductivity detector could detect each gas separately. The analytical precision is $\pm 0.1\%$ (<http://www.isotope.uottawa.ca/techniques/quantitative-analysis.html#vario>).

Py-FIMS

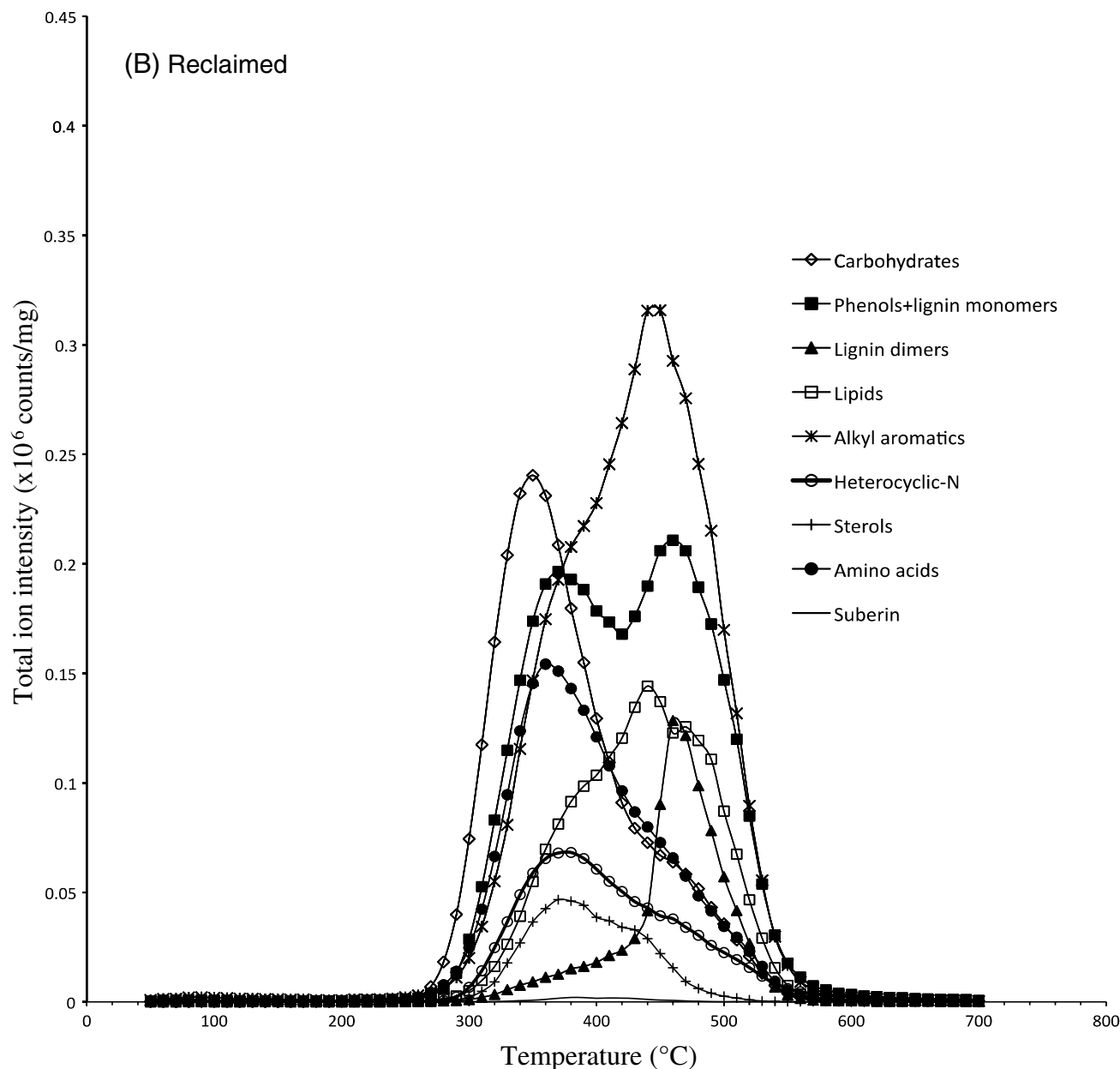
The SOM composition in samples collected from the 0–5 cm depth in the native, reclaimed, and reference eroded soil samples was investigated by Py-FIMS. Py-FIMS is a soft-ionization mass spectrometric method, which means there is little fragmentation, so that most signals volatilized during pyrolysis from the soil sample are molecular ions. Briefly, 1 mg of sample was air-dried in a sample tube and then heated in the direct inlet system of a double-focusing mass spectrometer

(Finnigan MAT 731, Bremen) under high vacuum (1×10^{-4} Pa) from 50 to 700 °C at a programmed linear heating rate of $10^\circ\text{C min}^{-1}$. Sixty mass spectra were recorded over the mass range m/z 15–900 Da. The signals in all spectra were integrated and plotted to yield a summed spectrum (Sorge et al. 1993). For example, Figs. 1A–1C show that the total ion intensities (TII), normalized to 1 mg sample mass, were plotted against pyrolysis temperatures to yield thermograms (Schnitzer and Monreal 2011).

Identification of mass spectrometric signals

The ion intensity of each mass spectrometric signal was computed from the mass spectra. The sum of all IIs was referred to as TIIs. The II of each signal identified

Fig. 2 (continued).



was a semiquantitative estimate of its concentration. Identifications of the major signals in the Py-FIMS spectra were based on comparisons with data published in the literature and, when available, on compounds with known chemical structures.

Analysis of sugars and polysaccharides

The mass spectrometric method which we used for sugars has been previously reported by Schulten (1984) and Kögel et al. (1988). The following mass signals were used for hexoses: m/z 126, 144, and 162; for pentoses: m/z 114 and 132; and for polysaccharides: m/z 60, 72, 82, 84, 96, 98, 110, and 112. Hexoses include glucose, galactose, and mannose, while pentoses refer to arabinose and xylose.

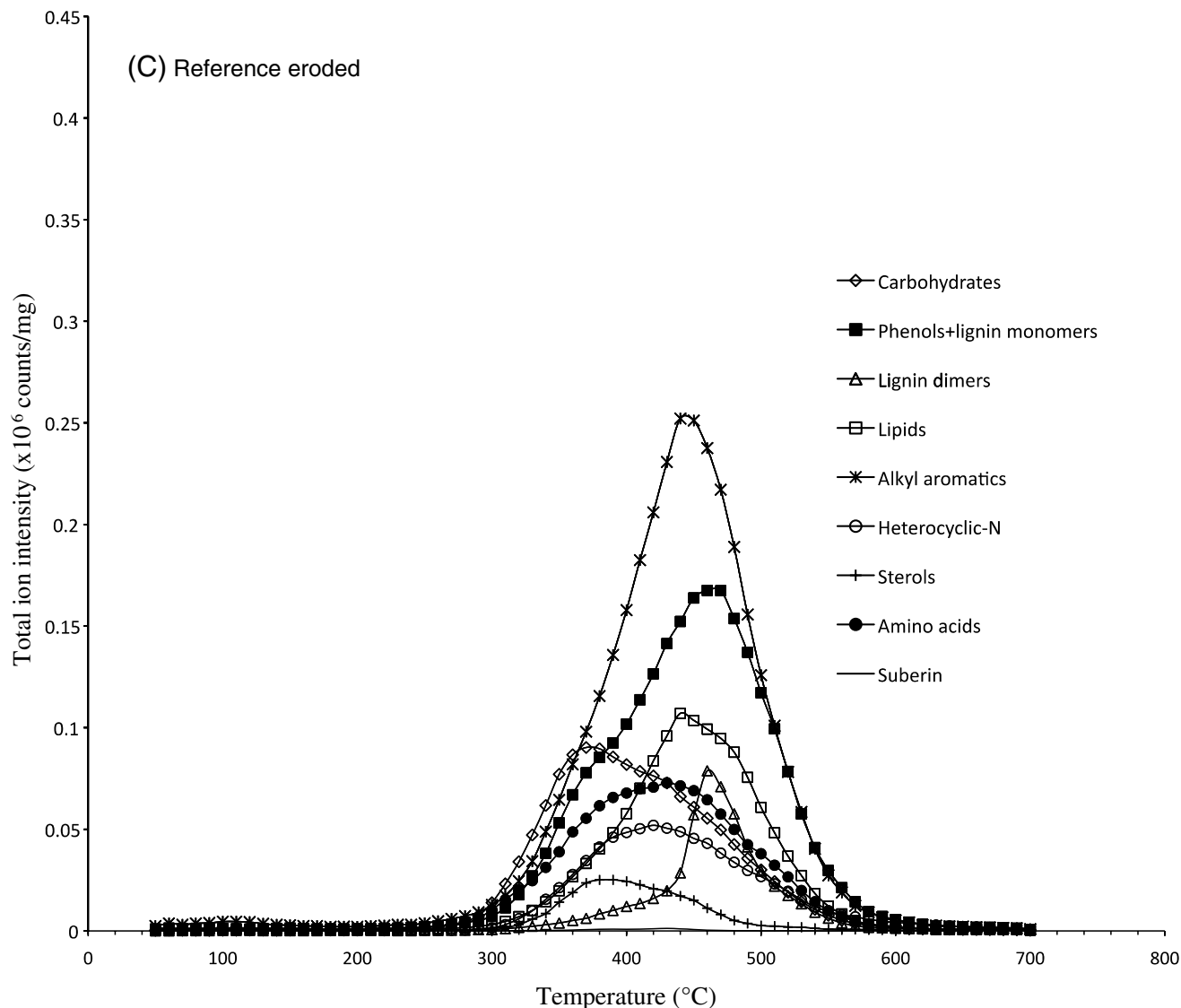
Identification of the remaining m/z signals

The identification of the m/z signals due to other chemical classes of compounds was described previously by Hempfling and Schulten (1990), Schnitzer and Schulten (1992), Sorge et al. (1993), Schnitzer and Monreal (2011), Monreal and Schnitzer (2013). Additional m/z values were identified with the help of the NIST chemical webbook (<http://webbook.nist.gov>) of the National Institute of Standards and Technology of the USA.

Statistical analyses

Analysis of variance (ANOVA) was conducted to determine significant differences in the content of soil inorganic and organic elements in the three Oxisol

Fig. 2 (concluded).



established treatments (Ferreira 2008). Paired *t* tests were run to determine the significance level of differences of the mean values for each of the chemical classes of compounds observed between the native, reclaimed, and eroded soil management treatments.

Results

Soil texture

The native and reclaimed soils were sandy clay loam and the reference eroded soil was sandy loam. The content of clay in the native soil was 281 g kg⁻¹, in the reclaimed soil it was 289 g kg⁻¹, and 163 g kg⁻¹ in the reference eroded samples. The content of sand was 597 g kg⁻¹ in the native, 642 g kg⁻¹ in the reclaimed soil, and 775 g kg⁻¹ in the reference eroded samples. The content of silt was 122 g kg⁻¹ in the native, 69 g kg⁻¹ in the reclaimed, and 62 g kg⁻¹ in the reference eroded soil samples.

Inorganic soil components

Table 1 shows the content of Fe, Fe₂O₃, SiO₂, and the Al+H species in the soil samples collected from the 0–5 cm depth of the three treatments. With the exception of Al+H species, the content of the inorganic elements and their mineral structures in soil samples were similar between the three soil treatments. The content of Al+H decreased in the following order: native > reclaimed > eroded.

Carbon and N content in soil and sewage sludge

The total content of C and N (% w/w, t ha⁻¹) in the top 5 cm of the three Oxisol treatments is shown in Table 1. The samples from the native site showed significantly higher content of both elements than the reclaimed and reference eroded soil samples. According to Tukey's test, the amounts of C and N in the reclaimed and reference eroded soil were similar, although their

Table 2. Ion intensities for m/z assigned to carbohydrates in samples obtained from the 0–5 cm depth of native and reclaimed phases relative to a reference eroded Oxisol.

m/z	Ion intensity (counts mg^{-1})		
	Native	Reclaimed	Reference eroded
Hexoses			
126	52798	56 214	23 709
144	94 943	97 576	92 222
162	116 709	151 607	47 917
Subtotal	264 449	305 397	163 848
Pentoses			
114	37 821	44 978	13 814
132	90 088	96 573	63 013
Subtotal	90 088	96 573	63 013
Polysaccharides			
60	54 801	56 672	10 828
72	75 037	45 704	47 191
82	154 835	145 830	113 551
84	104 600	125 993	61 341
96	332 987	397 660	166 354
98	80 093	102 934	35 030
110	193 787	240 731	94 484
112	90 614	104 080	50 541
Subtotal	1 086 752	1 219 502	579 319
Total*	1 441 288	1 621 471	806 179

*t test (Total): native vs reclaimed $p = 0.011$; native vs reference eroded $p = 0.0001$; reclaimed vs reference eroded $p = 0.0004$.

content tended to be higher in the reclaimed than in the eroded soil after 8 years of soil reclamation. The C/N ratio of SOM was near 15 in the reference eroded and reclaimed

samples, and 17 in the native soil samples, indicating a relatively higher degree of C decomposition and humification of OM in the native than in the other two Oxisol treatments. The concentration of C and N in the added sewage sludge was 206 and 71.3 g kg^{-1} soil (dry basis), respectively. The annual production of *Urochloa decumbens* dry matter in the reclaimed soil was 25 672 kg ha^{-1} . Although the annual production of dry plant matter was not measured in the native Oxisol, the range in production for aboveground biomass in a Cerrado biome with predominance of clayey Oxisol is similar to that measured in the reclaimed treatment (Lannes et al. 2012).

Thermal stability of SOM during sample pyrolysis

The thermal volatilization pattern of the total SOM in the native, reclaimed, and reference eroded Oxisol

Table 3. Ion intensities for m/z assigned to amino acids in samples obtained from the 0–5 cm depth of native and reclaimed phases relative to a reference eroded Oxisol.

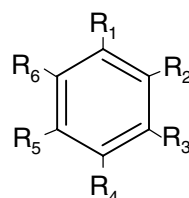
m/z	Ion intensity (counts mg^{-1})		
	Native	Reclaimed	Reference eroded
Acidic amino acids			
70	135 044	136 972	97 249
84	104 600	125 993	61 341
97	88 728	127 601	48 701
99	42 113	63 707	17 072
115	12 472	11 452	4 042
Subtotal	382 957	465 725	228 405
Neutral amino acids			
57	29 551	27 503	13 767
73	27 043	30 954	17 395
75	7 132	8 197	2 654
87	9 289	12 475	5 517
Subtotal	73 015	79 129	39 333
Neutral aromatic amino acids			
74	15 106	16 789	4 296
91	3 662	3 309	1 567
120	52 331	58 320	58 088
135	44 592	52 402	26 795
Subtotal	115 690	130 819	90 746
Basic amino acids			
129	27 128	19 598	21 903
135	44 592	52 402	26 795
Subtotal	71 720	72 000	48 698
Total*	643 381	747 673	407 780

*t test (total): native vs reclaimed $p = 0.020$; native vs reference eroded $p = 0.0005$; reclaimed vs reference eroded $p = 0.0015$.

during sample pyrolysis is shown in the upper right corner of Figs. 1A–1C. The pyrolysis of the native Oxisol produced the highest intensity maximum exothermic volatilization peak near 450 °C with a slight shoulder near ~500 °C (Fig. 1A). In comparison, the pyrolysis of the reclaimed soil samples produced an intermediate intensity exothermic volatilization peak near 380–390 °C, and a second maximum exothermic peak occurred near 450–460 °C (Fig. 1B). In the reference eroded samples, the single maximum exothermic volatilization peak of relatively lower intensity occurred near 460 °C (Fig. 1C). In this article, we defined thermolabile SOM as being represented by maximum peaks that volatilized at <440 °C and thermostable SOM by maximum peaks that volatilized at >450 °C (Monreal et al. 1997).

Table 4. Chemical structures for m/z assigned to phenols and lignin monomers in samples obtained from the 0–5 cm depth of native and reclaimed phases relative to a reference eroded Oxisol.

m/z	Structure	R_1	R_2	R_3	R_4	R_5	R_6
94		—OH	—H	—H	—H	—H	—H
108		—OH	—CH ₃	—H	—H	—H	—H
110		—OH	—OH	—H	—H	—H	—H
122		—OH	—CH ₃	—CH ₃	—H	—H	—H
124		—H	—H	—OCH ₃	—OH	—H	—H
126		—H	—H	—OH	—OH	—OH	—H
138		—CH ₃	—H	—OCH ₃	—OH	—H	—H
140		—OH	—H	—OCH ₃	—OH	—H	—H
150		—CH=CH ₂	—H	—OCH ₃	—OH	—H	—H
152		—CHO	—H	—OCH ₃	—OH	—H	—H
154		—H	—H	—OCH ₃	—OH	—OCH ₃	—H
164		—CH ₂ —CH=CH ₂	—H	—OCH ₃	—OH	—H	—H
166		—CH ₂ —CH ₂ —CH ₃	—H	—OCH ₃	—OH	—H	—H
168		—COOH	—H	—OCH ₃	—OH	—H	—H
178		—CH=CH—CHO	—H	—OCH ₃	—OH	—H	—H
180		—CH=CH—CH ₂ OH	—H	—OCH ₃	—OH	—H	—H
182		—CHO	—H	—OCH ₃	—OH	—OCH ₃	—H
194		—CH=CH—COOH	—H	—OCH ₃	—OH	—OCH ₃	—H
196		—CH ₂ —CHO	—H	—OCH ₃	—OH	—OCH ₃	—H
208		—CH=CH—CHO	—H	—OCH ₃	—OH	—OCH ₃	—H
210		—CH=CH—CH ₂ OH	—H	—OCH ₃	—OH	—OCH ₃	—H
212		—CH ₂ —COOH	—H	—OCH ₃	—OH	—OCH ₃	—H



The Py-FIMS analysis shows that the thermolabile and thermostable pools of SOM comprised different chemical classes of compounds (Tables 2–16). In all three Oxisol phases, the chemical classes contributing to the thermostable OM pool at >450 °C are mostly alkylaromatics, lipids, phenols+lignin monomers, lignin dimers, and *N*-heterocyclics (Figs. 2A–2C). In addition, lipids and *N*-heterocyclics showed a second thermostable shoulder component at >500 °C, especially in the native soil (Fig. 2A). Molecular examples of the thermostable SOM involved various derivatives of alkylbenzene, saturated and unsaturated fatty acids and alkanes, various phenols and lignin monomers, biphenyls, and phenylcoumarans (Tables 4, 7, 8, and 11).

Chemical classes of compounds contributing to the volatilization of the thermolabile pools of SOM involved carbohydrates with an exothermal maximum peak near 320 °C, and contributions of amino acids and sterols were observed from 390 to 400 °C (Figs. 2A–2C).

Mass spectrometry of SOM

The Py-FIMS spectra of the native, reclaimed, and eroded soils are shown in Figs. 1A–1C, respectively. Each of the three spectra extends from m/z 10 to m/z 500, where m/z signals are well separated from each other. Noteworthy, the volatilized OM from the three soil samples appear to be free of relatively high molecular weight

compounds (i.e., alkyl esters), which would be expected in the 600–900 m/z region.

We identified 12 chemical classes of compounds in each of the three soil treatments. These are listed in Tables 2–16 along with the ion intensities (IIs) for each organic compound identified in each class. The IIs stand for abundance of the organic molecular ions that were volatilized during pyrolysis. The chemical classes identified were carbohydrates, amino acids, phenols+lignin monomers, lignin dimers, alkyl aromatics (alkylbenzenes), flavonoids, *n*-alkanes+*n*-fatty acids (lipids), *n*-diols, *N*-heterocyclics, nitriles, sterols+steroids, and esters of suberins. The alkyl radicals are not considered a class by themselves, as they are formed during pyrolysis of long-chain aliphatics existing in SOM. In terms of the total chemical classes recovered from each Oxisol treatment, the Py-FIMS analysis of samples reported 32.8×10^6 counts mg^{-1} in the native samples, 29.4×10^6 counts mg^{-1} in the reclaimed samples, and 18.2×10^6 counts mg^{-1} in the reference eroded samples. In terms of the total chemical classes identified, these values correspond to 75% for the native soil, 67% for the reclaimed soil, and 42% for the reference eroded soil (Table 16). Overall, the abundance of chemical classes of compounds in all three Oxisol treatments decreased in the following order: lipids > *N*-heterocyclics >> *n*-alkylbenzenes > phenols+lignin monomers > *n*-diols > lignin dimers > carbohydrates > flavonoids > amino

Table 5. Ion intensities for m/z assigned to phenols and lignin monomers in samples obtained from the 0–5 cm depth of native and reclaimed phases relative to a reference eroded Oxisol.

		Ion intensity (counts mg ⁻¹)		
		Reference		
m/z	Identity	Native	Reclaimed	eroded
		Phenols		
94	Phenol	116 268	114 839	118 598
108	Methylphenol	84 084	95 507	77 294
110	Dihydroxybenzene	129 121	160 487	62 989
122	Dimethylphenol	56 245	69 147	38 283
124	Guaiacol	73 134	84 598	33 895
126	Trihydroxybenzene	52 796	56 214	23 708
138	Methylguaiacol	43 030	50 423	19 469
140	Hydroxyguaiacol	48 619	49 933	34 419
150	Ethyleneguaiacol	79 823	115 765	35 809
152	Vanillin	34 439	42 404	17 818
154	Syringol	70 368	57 952	59 375
Subtotal		787 997	897 269	521 656
		Lignin monomers		
164	Guaiacylpropene	65 657	81 401	24 786
166	Guaiacylpropane	59 811	52 287	39 235
168	Vanillic acid	143 365	117 477	108 663
178	Coniferyl aldehyde	88 235	64 895	50 340
180	Coniferyl alcohol	102 759	83 979	69 750
182	Syringyl aldehyde	189 453	176 000	139 604
194	Ferulic acid	313 404	267 392	209 538
196	Syringyl acetaldehyde	145 112	131 489	87 098
208	Sinapyl aldehyde	370 050	334 795	233 065
210	Sinapyl alcohol	157 826	156 549	94 258
212	Syringyl acetic acid	71 395	68 334	39 608
Subtotal		1 707 067	1 534 597	1 095 944
Total*		2 495 064	2 431 866	1 617 600

* t test (total): native vs reclaimed $p = 0.25$; native vs reference eroded $p < 0.0001$; reclaimed vs reference eroded $p < 0.0001$.

acids > nitriles and other N compounds > sterols+steroids > alkyl radicals >>> esters of suberin (Table 16).

An inspection of the mass spectrometry data in Tables 2–16 shows that relative to the reference eroded Oxisol, the abundance of most chemical classes of compounds was often highest in the native samples, followed by those in the reclaimed soil samples. Interestingly, the abundance of carbohydrates and amino acids were highest in the reclaimed soil (Table 2). The reference eroded samples had the lowest abundance of chemical classes of compounds. According to pairwise t test comparisons, the native soil samples had the highest abundance of lignin dimers, n -alkylbenzenes, flavonoids, n -diols, N -heterocyclics, nitriles, alkyl radicals, and sterols+steroids. The

Table 6. Chemical structures for m/z assigned to lignin dimers in samples obtained from the 0–5 cm depth of native and reclaimed phases relative to a reference eroded Oxisol.

<i>m/z</i>	Structure	<i>R</i> ₁	<i>R</i> ₂
<u>Biphenyl</u>			
246		—H	—H
260		—CH ₃	—H
272		—CH ₃	—CH ₃
274		—CH ₂ CH ₃	—H
286		—CH=CH—CH ₃	—H
300		—CH=CH—CH ₃	—CH ₃
302		—CH=CH—CH ₂ —OH	—H
316		—CH=CH—CH ₂ —OH	—CH ₃
328		—CH=CH—CH ₂ —OH	—CH=CH ₂
<u>Phenylcoumaran</u>			
314		—CH—CH—OH	—H
330		—CH ₂ —OH	—OCH ₃
332		—CH ₂ —OH	—OCH ₃
340		—CH=CH—CH ₃	—OCH ₃
342		—CH=CH—CH ₃	—OCH ₃
346		—CH ₂ —CH ₂ —OH	—OCH ₃
356		—CH=CH—CH ₂ —OH	—OCH ₃
358			—CH=CH—CH ₂ —OH

abundance of phenols + lignin monomers, lipids, alkyl radicals, N -heterocyclics, and esters of suberin was the same in the native and the reclaimed soil samples (Tables 2–16).

Lipids and N -heterocyclics are by far the most abundant classes of compounds, with 20–480 times more content than the other chemical classes in the three Oxisol phases. Of the total identified m/z signals, lipids and heterocyclic- N comprised 26 and 19% in the native soil, 21 and 18% in the reclaimed soil, versus 14 and 11% in the reference eroded soil, respectively. The abundance of lipids and heterocyclic- N was followed by the abundance of lignin monomers and alkylaromatics, which were highest in the native > reclaimed > reference eroded soil. The abundance of lignin monomers and alkylaromatics was similar and ranged from 5 to 5.9% in the native and reclaimed soil samples, versus 3.5 to 3.7% in the reference eroded samples, respectively (Table 16).

The other seven classes of compounds contributed to less than 3.5% of the total IIs in the three soils, with their abundance usually highest in the native > reclaimed > reference eroded samples. For example, the abundance of sterols, steroids, and esters of suberin represented less than 1% of the total identified m/z signals (Tables 14 and 15). The latter compound classes are important components of humic substances, plants, soil fungi, and roots. The abundance of these three classes was always highest in the native soil samples. The signals of cholestine (m/z 370), cholesterol (m/z 386), stigmastine (m/z 394), and campesterol (m/z 400) were the main contributors

Table 7. Ion intensities for m/z assigned to lignin dimers in samples obtained from the 0–5 cm depth of native and reclaimed phases relative to a reference eroded Oxisol.

	Ion intensity (counts mg ⁻¹)		
<i>m/z</i>	Native	Reclaimed	Reference eroded
Biphenyls			
246	158 684	148 805	88 251
260	141 035	113 526	80 834
270	106 192	111 130	51 020
272	110 690	102 226	61 494
274	127 295	101 295	78 951
286	59 825	48 794	32 505
298	110 089	109 307	53 732
300	68 802	59 427	36 795
302	67 135	46 687	40 487
312	45 823	47 863	20 972
316	81 242	58 347	46 459
328	41 095	33 487	23 326
Subtotal	1 104 829	965 372	607 009
Phenylcoumarans			
314	53 623	45 350	30 168
330	60 179	44 897	35 185
332	31 338	61 844	42 745
340	28 619	22 523	12 937
342	31 704	27 171	16 574
346	52 730	50 045	34 499
356	53 323	44 034	27 638
358	39 217	25 949	21 675
Subtotal	390 217	321 812	221 421
Total*	1 495 556	1 287 184	828 430

*t test (total): native vs reclaimed $p = 0.009$; native vs reference eroded $p < 0.0001$; reclaimed vs reference eroded $p = 0.0001$.

to the abundance of sterols and steroids of plant origin. The signals at m/z 432 and m/z 446 were the main contributors to esters of suberin, denoting the presence of root cell components. Ergosterol at m/z 396 represents a fingerprint for soil fungi, and it was highest in the native > reclaimed > reference eroded soil.

Contribution of individual m/z signals to key chemical classes

In the native and reclaimed Oxisol samples, the amounts of carbohydrates was closely associated with the content of hexoses and polysaccharides, and that of amino acids was associated with the content of acidic and aromatic amino acids (Tables 2 and 3).

Lignin monomers were the main contributor (68%) to the total abundance of phenol+lignin monomer class (Tables 4 and 5), with synapyl aldehyde, ferulic acid, syringyl aldehyde, and sinapyl alcohol being the four

Table 8. Ion intensities for m/z assigned to n -alkyl benzenes in samples obtained from the 0–5 cm depth of native and reclaimed phases relative to a reference eroded Oxisol.

m/z	Identity	Ion intensity (counts mg^{-1})		
		Native	Reclaimed	Reference eroded
92	Methylbenzene	116 539	63 506	75 870
106	Ethylbenzene	92 663	62 036	86 544
120	Propylbenzene	52 330	58 319	58 088
134	Butylbenzene	89 898	101 976	78 831
148	Pentylbenzene	92 816	107 131	62 269
162	Hexylbenzene	116 709	151 607	47 917
176	Heptylbenzene	97 023	115 997	41 022
190	Octylbenzene	109 879	114 651	47 910
204	Nonylbenzene	183 693	163 464	96 067
218	Decylbenzene	315 741	277 291	187 496
232	Undecylbenzene	332 837	300 947	200 615
246	Dodecylbenzene	158 684	148 805	88 250
260	Tridecylbenzene	141 034	113 526	80 834
274	Tetradecylbenzene	127 295	101 295	78 950
288	Pentadecylbenzene	108 994	81 594	69 372
302	Hexadecylbenzene	67 135	46 687	40 487
316	Heptadecylbenzene	81 242	58 347	46 459
330	Octadecylbenzene	60 178	44 896	35 185
344	Nonadecylbenzene	95 432	69 795	48 044
358	Cosylbenzene	39 217	25 948	21 675
372	Uncosylbenzene	65 669	46 157	34 912
386	Docosylbenzene	45 504	19 588	17 267
Total*		2 590 512	2 273 563	1 544 064

*t test (total): native vs reclaimed $p = 0.002$; native vs reference eroded $p < 0.0001$; reclaimed vs reference eroded $p = 0.0002$.

most abundant lignin monomers. Biphenyls contributed the most to the abundance of lignin dimers and they were almost 2.8 times greater than phenylcoumarans, with m/z 246 and m/z 260 being the most abundant organic species (Tables 6 and 7). The n -alkylbenzene class was dominated by the abundance of undecylbenzene (m/z 232) and decylbenzene (m/z 218) species, followed by dodecylbenzene (m/z 246) and tridecylbenzene (m/z 260), and other m/z signals (Table 8). Table 9 shows that flavanone (m/z 224) and flavone (m/z 222) were the most abundant m/z signals, with a concentration 2–3 times higher than the other five flavonoids. Alcohols such as those shown in signals m/z 230 ($n\text{-C}_{14}$), m/z 216 ($n\text{-C}_{13}$), m/z 244 ($n\text{-C}_{15}$), and m/z 258 ($n\text{-C}_{16}$) were the most abundant diols (Table 10).

Within the soil lipid class, the unsaturated fatty acids (USFAs) with two or more double bonds were the most abundant group of compounds, followed by saturated fatty acids (SFAs), and a group of m/z signals including alkanes and unsaturated fatty acids (Table 11). The USFAs with two or more bonds were almost twice as abundant as the SFAs, and the USFAs with one double

Table 9. Ion intensities for m/z assigned to flavonoids in samples obtained from the 0–5 cm depth of native and reclaimed phases relative to a reference eroded Oxisol.

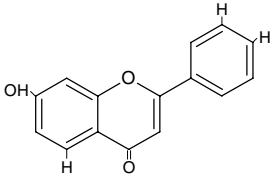
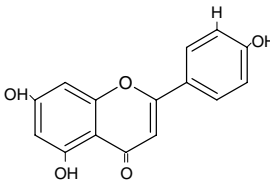
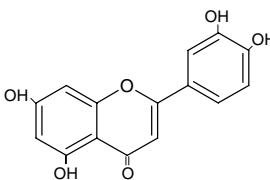
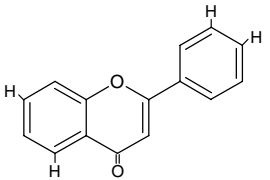
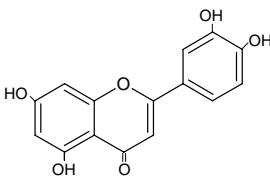
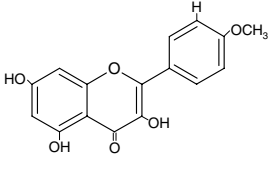
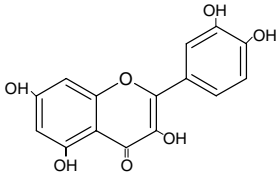
Structure	Ion intensity (counts mg^{-1})		
	Native	Reclaimed	Reference eroded
Flavones			
Flavone, MW = 222			
	360 124	336 701	201 844
Apigenin, MW = 270			
	106 192	111 130	51 020
Luteolin, MW = 286			
	59 824	48 794	32 505
Flavanones			
Flavonone, MW = 224			
	310 280	285 218	198 447
Eriodictyol, MW = 288			
	108 993	81 594	69 372
Flavonols			
Kaempferide, MW = 299			
	40 006	42 926	14 955

Table 9 (concluded).

Structure	Ion intensity (counts mg^{-1})		
	Native	Reclaimed	Reference eroded
Quercetin, MW = 302			
	67 135	46 687	40 488
Total*	1 082 467	977 447	624 883

*t test (total): native vs reclaimed $p = 0.016$; native vs reference eroded $p = 0.009$; reclaimed vs reference eroded $p = 0.0170$.

Table 10. Ion intensities for m/z assigned to n -diols in samples obtained from the 0–5 cm depth of native and reclaimed phases relative to a reference eroded Oxisol.

m/z	Identity	Ion intensity (counts mg^{-1})		
		Native	Reclaimed	Reference eroded
202	$n\text{-C}_{12}$	248 657	174 485	135 505
216	$n\text{-C}_{13}$	382 946	285 234	237 077
230	$n\text{-C}_{14}$	422 629	350 245	246 606
244	$n\text{-C}_{15}$	365 081	342 679	223 536
258	$n\text{-C}_{16}$	277 507	280 297	156 887
272	$n\text{-C}_{17}$	110 689	102 226	61 493
286	$n\text{-C}_{18}$	59 824	48 793	32 505
300	$n\text{-C}_{19}$	137 604	118 854	73 590
314	$n\text{-C}_{20}$	53 623	45 350	30 168
328	$n\text{-C}_{21}$	41 095	33 487	23 325
342	$n\text{-C}_{22}$	31 703	27 170	16 574
Total*		2 062 558	1 749 390	1 200 476

*t test (total): native vs reclaimed $p = 0.0090$; native vs reference eroded $p = 0.0005$; reclaimed vs reference eroded $p = 0.0013$.

bond. Among the USFA with two or more double bonds, heptadecadienoic acid ($\text{C}_{17:2}$, m/z 266), hexadecadienoic acid ($\text{C}_{16:2}$), eicosadienoic acid ($\text{C}_{20:2}$, m/z 308), linoleic acid ($\text{C}_{18:2}$, m/z 280), together with pentadecadienoic ($\text{C}_{15:2}$, m/z 238) and tetradecadienoic acid ($\text{C}_{14:2}$, m/z 224) were the five most abundant species. We assumed that alkanes and USFs with one double bond contributed each with 50% of the measured abundance for each assigned m/z ; as the Py-FIMS analytical technique could not separate their exact contributions. Among the SFAs, lauric acid ($n\text{-C}_{12}$, m/z 200), myristic acid ($n\text{-C}_{14}$, m/z 228), $n\text{-C}_{15}$, palmitic acid ($n\text{-C}_{16}$, m/z 256), and margaric acid

Table 11. Ion intensities for m/z assigned to fatty acids and n -alkanes in the 0–5 cm depth of native and reclaimed phases relative to a reference eroded Oxisol.

m/z	Fatty acid	n -Alkane	Ion intensity (counts mg^{-1})		
			Native	Reclaimed	Reference eroded
46	$n\text{-C}_1$		16 798	6 727	2924
58	$n\text{-C}_{2:1}$	$n\text{-C}_4$	495 252	263 503	297 207
60	$n\text{-C}_2$		54 801	56 571	10 828
72	$\text{C}_{3:1}$	$n\text{-C}_5$	50 024	30 469	31 461
74	$n\text{-C}_3$		15 106	16 789	4 295
86	$\text{C}_{4:1}$	$n\text{-C}_6$	91 725	89 170	38 338
88	$n\text{-C}_4$		6 799	10 219	2 443
100	$\text{C}_{5:1}$	$n\text{-C}_7$	34 849	41 326	14 669
102	$n\text{-C}_5$		7 585	10 597	3 055
114	$\text{C}_{6:1}$	$n\text{-C}_8$	37 821	44 978	13 814
116	$n\text{-C}_6$		29 027	24 385	27 052
128	$\text{C}_{7:1}$	$n\text{-C}_9$	80 123	56 035	63 251
130	$n\text{-C}_7$		26 135	18 349	28 632
142	$\text{C}_{8:1}$	$n\text{-C}_{10}$	93 871	69 404	79 725
144	$n\text{-C}_8$		94 943	978 576	92 222
156	$\text{C}_{9:1}$	$n\text{-C}_{11}$	123 893	82 197	100 509
158	$n\text{-C}_9$		108 738	117 679	81 408
170	$\text{C}_{10:1}$	$n\text{-C}_{12}$	184 828	120 676	117 237
172	$n\text{-C}_{10}$		123 250	128 370	73 065
182	$\text{C}_{11:2}$		189 453	176 000	139 604
184	$\text{C}_{11:1}$	$n\text{-C}_{13}$	236 688	175 064	140 268
186	$n\text{-C}_{11}$		125 105	105 363	40 300
196	$\text{C}_{12:2}$		145 112	131 489	87 098
198	$\text{C}_{12:1}$	$n\text{-C}_{14}$	288 695	205 205	133 264
200	$n\text{-C}_{12}$		220 840	204 359	69 024
210	$\text{C}_{13:2}$		157 826	156 548	94 257
212	$\text{C}_{13:1}$	$n\text{-C}_{15}$	71 395	68 334	39 608
214	$n\text{-C}_{13}$		153 361	158 214	51 133
224	$\text{C}_{14:2}$		310 280	285 218	198 447
226	$\text{C}_{14:1}$	$n\text{-C}_{16}$	214 664	204 100	119 196
228	$n\text{-C}_{14}$		236 725	188 645	116 259
238	$\text{C}_{15:2}$		314 719	280 965	172 700
240	$\text{C}_{15:1}$	$n\text{-C}_{17}$	221 109	201 497	132 267
242	$n\text{-C}_{15}$		252 669	222 139	126 448
252	$\text{C}_{16:2}$		457 996	327 481	244 732
254	$\text{C}_{16:1}$	$n\text{-C}_{18}$	268 295	236 022	163 315
256	$n\text{-C}_{16}$		242 264	232 007	119 088
266	$\text{C}_{17:2}$		542 355	370 542	306 087
268	$\text{C}_{17:1}$	$n\text{-C}_{19}$	239 034	191 078	144 635
270	$n\text{-C}_{17}$		212 383	222 260	102 040
278	$\text{C}_{18:3}$		298 698	225 786	144 591
280	$\text{C}_{18:2}$		371 046	267 946	225 979
282	$\text{C}_{18:1}$	$n\text{-C}_{20}$	198 508	166 930	111 306
284	$n\text{-C}_{18}$		148 232	141 286	70 517
292	$\text{C}_{19:3}$		207 518	188 041	111 082
294	$\text{C}_{19:2}$		277 281	227 791	158 532
296	$\text{C}_{19:1}$	$n\text{-C}_{21}$	155 177	131 578	89 524
298	$n\text{-C}_{19}$		110 089	109 307	53 732
306	$\text{C}_{20:3}$		186 194	171 196	96 779
308	$\text{C}_{20:2}$		368 270	288 894	158 715
310	$\text{C}_{20:1}$	$n\text{-C}_{22}$	131 254	105 857	61 246
312	$n\text{-C}_{20}$		45 822	47 862	20 972
320	$\text{C}_{21:3}$		132 179	123 690	66 721

Table 11 (concluded).

m/z	Fatty acid	n -Alkane	Ion intensity (counts mg^{-1})		
			Native	Reclaimed	Reference eroded
322	$\text{C}_{21:2}$		179 456	148 969	95 427
324	$\text{C}_{21:1}$	$n\text{-C}_{23}$	100 856	75 004	26 009
326	$n\text{-C}_{21}$		63 811	60 820	31 918
334	$\text{C}_{22:3}$		111 857	97 567	57 577
336	$\text{C}_{22:2}$		189 947	214 167	82 077
338	$\text{C}_{22:1}$	$n\text{-C}_{24}$	85 010	68 449	42 025
340	$n\text{-C}_{22}$		28 618	22 523	12 937
352	$\text{C}_{23:1}$	$n\text{-C}_{25}$	60 184	42 524	30 751
354	$n\text{-C}_{23}$		44 108	36 108	19 715
366	$\text{C}_{24:1}$	$n\text{-C}_{26}$	60 114	43 448	25 181
368	$n\text{-C}_{24}$		67 212	45 236	23 987
380	$\text{C}_{25:1}$	$n\text{-C}_{27}$	55 760	34 536	18 265
382	$n\text{-C}_{25}$		59 237	35 748	14 572
394	$\text{C}_{26:1}$	$n\text{-C}_{28}$	62 113	14 832	5 476
396	$n\text{-C}_{26}$		37 732	23 768	7 613
408	$\text{C}_{27:1}$	$n\text{-C}_{29}$	49 394	35 642	9 286
410	$n\text{-C}_{27}$		19 755	10 474	5 455
422	$\text{C}_{28:1}$	$n\text{-C}_{30}$	18 501	12 959	5 191
424	$n\text{-C}_{28}$		14 851	10 346	4 264
436	$\text{C}_{29:1}$	$n\text{-C}_{31}$	8 912	8 032	3 469
438	$n\text{-C}_{29}$		9 323	3 589	2 368
450	$\text{C}_{30:1}$	$n\text{-C}_{32}$	5 198	3 324	1 979
452	$n\text{-C}_{30}$		4 971	3 803	1 348
464	$\text{C}_{31:1}$	$n\text{-C}_{33}$	2 435	2 496	1 055
466	$n\text{-C}_{31}$		2 080	1 983	1 210
478	$\text{C}_{32:1}$	$n\text{-C}_{34}$	1 517	2 003	621
480	$n\text{-C}_{32}$		1 576	1 832	670
492	$\text{C}_{33:1}$	$n\text{-C}_{35}$	1 270	1 151	1 003
494	$n\text{-C}_{33}$		560	917	680
Type of fatty acid on n -alkane					
Saturated n -fatty acid			2 785 227	2 506 066	1 287 979
Unsaturated fatty acid with one double bond			1 957 458	1 471 679	1 082 303
Unsaturated fatty acid with \geq two double bonds			4 440 187	3 682 291	2 440 405
n -Alkanes			1 957 458	1 471 679	1 082 303
Total lipids*			11 140 330	9 131 715	5 892 990

*t test (total): native vs reclaimed $p = 0.156$; native vs reference eroded $p < 0.0001$; reclaimed vs reference eroded $p = 0.0001$.

($n\text{-C}_{17}$, m/z 270) were the most abundant species. The species of SFAs with chain lengths $< n\text{-C}_{10}$ and for $> n\text{-C}_{20}$ to $n\text{-C}_{33}$ were the least abundant fatty acids in all three Oxisol samples (Table 11). Table 12 shows that the alkyl radicals identified in the Oxisol ranged from ethyl to octyl, that is, from C_2 to C_8 . The concentration of alkyl radicals in the reference eroded samples was low ($\sim 158\,000$ counts mg^{-1}) $<$ reclaimed samples ($\sim 387\,000$ counts mg^{-1}) $<$ native samples ($\sim 523\,000$

Table 12. Ion intensities for m/z assigned to alkyl radicals in samples obtained from the 0–5 cm depth of native and reclaimed phases relative to a reference eroded Oxisol.

m/z	Identity	Ion intensities (count mg^{-1} soil)		
		Native	Reclaimed	Reference eroded
29	Ethyl	199 390	69 795	28 289
43	Propyl	291 972	208 986	70 783
57	Butyl	29 550	27 503	13 766
71	Pentyl	31 664	35 714	21 180
85	Hexyl	49 564	69 613	28 444
99	Heptyl	21 057	31 854	8 536
113	Octyl	16 051	20 818	8 720
Total*		522 856	387 345	158 120

*t test (total): native vs reclaimed $p = 0.147$; native vs reference eroded $p = 0.048$; reclaimed vs reference eroded $p = 0.027$.

counts mg^{-1}). These alkyl radicals are usually generated by chemical and (or) enzymatic reactions from aliphatic side chains bonded to long aliphatic chains, especially near double bonds, in fatty acids, alkanes, n -diols, and (or) n -alkyl esters. It is also possible that the free alkyl radicals were formed during pyrolysis or in the electro-magnetic field of the mass spectrometer.

The N -heterocyclics appeared as the second most abundant class of chemical compounds (Table 13). The abundance of N -heterocyclic groups decreased in the following order: pyrazole, substituted pyrazoles and imidazoles > pyrazines and substituted pyrazines > carbazole and substituted carbazoles > quinolines and benzoquinolines >> pyridine and substituted pyridines > indoles and substituted indoles > nitriles > phenylpyridine and substitutes. The first four groups of N -heterocyclics were from two to three times more abundant than the other five groups of N -heterocyclics identified in the three Oxisol treatments (Table 13). In the pyrazole and imidazoles group, methylpyrazole derivative species were the most abundant. Examples of the latter involves compounds such as hydroxypyrazole (m/z 84), dimethylpyrazole (m/z 96), and tetramethyl-heptylpyrazole (m/z 222). In all three soils and among the pyrazine and substituted pyrazines, pentamethyl-pentylpyrazine, pentamethyl-butylpyrazine, and pentamethyl-propylpyrazine were the most abundant species of all N -heterocyclic compounds. Various species involving methyl derivatives of carbazole, quinolines, phenylpyridines, and indoles were identified frequently and contributed most to the molecular abundance in the groups of N -heterocyclics (Table 13).

Discussion

Thermograms of OM volatilization are essentially differential thermal analysis curves, which provide

information on the thermal stability of chemical components in SOM during pyrolysis. Differences in the exothermic maxima of SOM volatilization indicate the degree to which components of different molecular complexity have been influenced by microbial processing and physicochemical associations of OM with inorganic components. For example, and in relative terms, the presence of a single thermostable component (>450 °C) in the native and reference eroded samples indicates that SOM is highly humified and decomposed and is strongly bound to clay minerals. In addition, the thermally stable SOM pool may also represent complex and polymerized chemical structures (Schnitzer and Monreal 2011). Conversely, the thermolabile peaks at 320 or <400 °C in the reclaimed soil samples indicates the SOM bound less strongly to clay minerals. The presence of thermolabile and less humified OM involving carbohydrates, amino acids, and sterols reflects to a large extent contributions to SOM from pools of fresh OM added via plant residues and sewage sludge in the reclaimed Oxisol.

In general, most SOM in thermolabile and thermostable pools is found in organo-mineral complexes in clay and aggregate fractions, and such OM cannot be separated easily from clay minerals, as reported by Chenu and Plante (2006). The association between organic and mineral constituents in microaggregate and clay fractions increases the turnover time of SOM (Monreal et al. 1997, 2010). Soil humic substances, which can make up 60–80% of the total SOM, are mostly stabilized as calcium humates and in reactions with crystalline and amorphous mineral and metal species. For example, the accumulation of humic substances in the fine clay fraction is favoured by expandable phyllosilicates in a Chernozemic soil of Canada (Schnitzer and Kodama 1977). In Podzolic soils, simple and mobile humic substances are preferentially bonded by Fe and aluminum inorganic species (Tyurin 1953). Oxisols in Brazil cover approximately 60% of its territory, have an acid pH, are highly weathered, and are dominated by variable-charge components, with relatively low amounts of SOM and variable clay content (Moreira et al. 2008; Ferreira et al. 2010).

In our research study, we focused on the chemical molecular components of OM in whole Oxisol samples. Although we did not study soil organo-mineral complexes in the Oxisol, we assumed that most OM was bound in stable organo-mineral complexes, especially associated with the mineral species of Fe, Al, and silicates of the Oxisol (Table 1). The studied Oxisol presented a high clay content, especially in the native and reclaimed samples, but clay was also present in the reference eroded soil. Complementary chemical analyses of key inorganic components show the presence of Fe, Al, and silicon (Si) mineral species and suggest that SOM in the Oxisol is mostly bound to these mineral species but is also bound to extractable species of Al oxide and

Table 13. Ion intensities for m/z assigned to *N*-heterocyclics in samples obtained from the 0–5 cm depth of native and reclaimed phases relative to a reference eroded Oxisol.

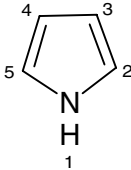
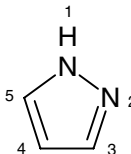
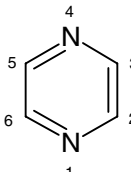
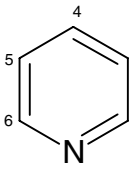
m/z	Structure	Identity	Ion intensity (counts mg ⁻¹)		
			Native	Reclaimed	Reference eroded
Substituted pyrroles					
67		Pyrrole	138 714	68 717	123 376
81		Methylpyrrole	113 539	81 701	113 197
83		Hydroxypyrrole	61 216	80 057	49 185
109		2-Acetylpyrrole	73 527	83 409	42 807
186		Diketopyrrole	125 105	105 363	40 299
Subtotal			512 101	419 247	368 865
Pyrazole and substituted pyrazoles and imidazoles					
68		Pyrazole	43 304	34 267	28 149
82		Methylpyrazole	154 835	145 830	113 551
84		Hydroxypyrazole	209 199	251 985	122 681
96		Dimethylpyrazole	332 986	397 660	166 353
110		1,3,5-Trimethylpyrazole	129 121	160 487	62 989
124		1-Ethyl-3,5-dimethylpyrazole	73 134	84 598	33 895
138		Pentamethylpyrazole	43 030	50 423	19 468
166		Tetramethyl-propylpyrazole	59 810	52 286	39 235
180		Tetramethyl-butylpyrazole	102 759	83 979	69 749
222		Tetramethyl-heptylpyrazole	360 124	336 701	201 844
99		4-Methylimidazole	21 056	31 853	8 536
130		2-Ethyl-4,5-dihydroxy-imidazole	26 134	19 598	21 902
Subtotal			1 604 395	1 670 014	933 504
Pyrazine and substituted pyrazines					
80		Pyrazine	45 585	31 771	42 025
108		2,3-Dimethylpyrazine	84 084	95 507	77 294
136		Tetramethylpyrazine	83 641	104 396	46 446
152		Methoxy-propylpyrazine	34 438	42 404	17 817
178		Pentamethyl-ethylpyrazine	88 235	64 895	50 340
192		Pentamethyl-propylpyrazine	272 403	244 179	165 454
206		Pentamethyl-butylpyrazine	337 010	293 149	229 884
220		Pentamethyl-pentylpyrazine	448 569	338 792	254 977
Subtotal			1 393 966	1 215 093	884 238
Pyridine and substituted pyridines					
79		Pyridine	76 501	36 585	44 446
93		Methylpyridine	90 407	55 518	77 384
94		Aminopyridine	116 268	114 839	118 597
95		3-Hydroxypyridine	90 605	95 245	66 177
104		3-Nitrile pyridine	53 656	45 095	42 113
107		Dimethylpyridine	59 506	45 425	51 177
111		Dihydroxypyridine	61 325	88 386	29 164
121		Trimethylpyridine	49 912	52 690	36 965
135		Tetramethylpyridine	44 592	52 402	26 795
149		Pentamethylpyridine	45 395	62 532	24 008
153		Hydroxy-acetoxypyridine	57 767	52 689	22 285
163		Hexamethylpyridine	39 118	49 394	13 121
177	Pentamethyl-ethylpyridine	32 593	42 847	11 685	

Table 13 (continued).

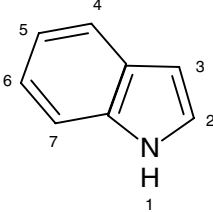
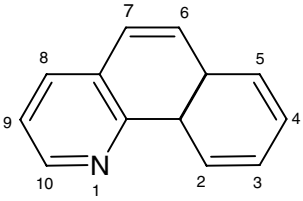
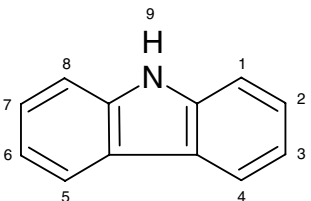
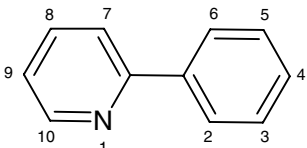
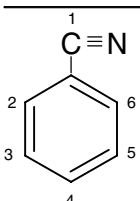
<i>m/z</i>	Structure	Identity	Ion intensity (counts mg ⁻¹)		
			Native	Reclaimed	Reference eroded
Subtotal			817 645	793 647	563 918
Indole and substituted indoles					
117		Indole	124 455	76 166	106 521
131		3-Methylindole	84 689	70 171	67 504
145		2,6-Dimethylindole	73,176	73 833	44 060
159		1,2,3-Trimethylindole	59 660	65 194	32 798
161		Indolethanol	48 916	64 072	22 633
173		Methyl-acetylindole	54 269	64 895	23 667
175		Indole acetic acid	49 463	63 687	18 273
187		Ethyl-acetylindole	76 988	88 936	21 105
201		Hexamethylindole	76 889	91 541	18 133
243		Hexamethyl-propylindole	127 831	144 784	45 674
Subtotal			776 336	803 279	400 368
Quinoline and substituted benzoquinolines					
155		Quinoline	18 085	13 065	14 601
133		Isoquinoline	56 943	64 648	43 507
157		Ethylquinoline	55 227	50 326	37 160
171		Propylquinoline	68 752	67 226	37 977
179		Benzoquinoline	56 117	50 237	28 238
185		Butylquinoline	78 840	85 842	37 439
193		Methylbenzoquinoline	94 031	89 840	49 781
207		Dimethylbenzoquinoline	117 469	116 679	65 532
221		Trimethylbenzoquinoline	147 950	136 419	68 115
235		Tetramethylbenzoquinoline	131 723	136 126	53 579
249		Pentamethylbenzoquinoline	114 229	111 293	38 973
263		Hexamethylbenzoquinoline	91 850	96 423	33 912
277		Heptamethylbenzoquinoline	81 609	75 000	24 897
291		Octamethylbenzoquinoline	52 218	58 306	22 880
Subtotal			1 201 213	1 177 651	585 795
Carbazole and substituted carbazoles					
167		Carbazole	96 909	105 177	51 459
181		Methylcarbazole	105 680	99 894	60 012
195		Dimethylcarbazole	139 192	138 785	71 745
209		Trimethylcarbazole	139 442	141 509	67 019
223		Tetramethylcarbazole	123 531	130 129	56 005
237		Pentamethylcarbazole	119 900	129 382	45 116
251		Hexamethylcarbazole	133 681	130 088	59 698
265		Heptamethylcarbazole	120 521	118 746	39 150
279		Octamethylcarbazole	85 043	76 915	37 214
293		Nonamethylcarbazole	68 115	71 029	30 799
307		Octamethyl-propylcarbazole	56 411	56 859	26 199
321		Octamethyl-butylcarbazole	42 321	48 667	20 996
335		Octamethyl-pentylcarbazole	33 584	34 425	14 821
349		Octamethyl-hexylcarbazole	24 697	28 287	11 840
Subtotal			1 289 297	1 309 892	592 068

Table 13 (concluded).

			Ion intensity (counts mg ⁻¹)		
m/z	Structure	Identity	Native	Reclaimed	Reference eroded
Phenylpyridine and substituted phenylpyridines					
155	<div>Phenylpyridine</div> 	Phenylpyridine	41 005	34 193	26 628
281		Nonamethylphenylpyridine	108 510	91 399	60 325
295		Decamethylphenylpyridine	87 160	75 584	42 835
309		Nonamethyl-propylphenylpyridine	114 880	85 601	45 535
323		Nonamethyl-propylphenylpyridine	51 877	50 122	30 414
337		Nonamethyl-butylphenylpyridine	56 153	69 924	27 438
351		Nonamethyl-pentylphenylpyridine	37 034	26 328	17 801
365		Nonamethyl-hexylphenylpyridine	35 656	24 911	14 954
379		Nonamethyl-heptylphenylpyridine	29 222	18 238	10 705
Subtotal			561 497	471 300	276 635
Nitrile and other N-compounds					
69	Nitriles	2-Methylpropanenitrile	43 304	34 267	28 149
87	$\text{R}-\text{C}\equiv\text{N}$	Formylacetamide	9 289	12 475	5 517
91		Cyanocyclopentadiene	3 661	3 308	1 567
97	Benzonitriles	4-Methylpentanenitrile	88 728	127 601	48 701
98		2,5-Pyrrolidinedione	80 092	102 933	35 030
103		Benzonitrile	117 585	39 368	54 623
113		Amino-methylfuranone	16 051	20 817	8 720
119		4-Hydroxybenzonitrile	39 463	42 929	32 508
122		Heptanedinitrile	56 245	69 146	38 283
129		1-Piperazineeethanamine	27 127	19 598	21 902
132		5-Methyl-1H-indazole	52 266	51 594	49 198
137		Amino-benzene-ethanol	73 657	108 340	23 739
Subtotal			607 470	632 379	347 938
Summary					
Pyrrole and substituted pyrroles			512 101	419 247	368 865
Pyrazole and substituted pyrazoles and imidazoles			1 604 395	1 670 014	933 504
Pyrazine and substituted pyrazines			1 393 966	1 215 093	884 238
Pyridine and substituted pyridines			817 645	793 647	563 918
Indoles and substituted indoles			776 336	803 279	400 368
Quinolines and benzoquinolines			1 201 213	1 177 651	585 795
Carbazole and substituted carbazoles			1 289 297	1 309 892	592 068
Phenylpyridine and substituted phenylpyridines			561 497	471 300	276 635
Nitriles and other N-compounds			607 470	632 379	347 938
Total* [†]			8 763 920	8 492 501	4 953 328

*t test for total N-heterocyclics: native vs reclaimed $p = 0.160$; native vs eroded $p < 0.0001$; reclaimed vs eroded $p < 0.0001$.

†t test for total nitriles: native vs reclaimed $p = 0.46$; native vs reference eroded $p < 0.0027$; reclaimed vs reference eroded $p = 0.0170$.

hydroxides. The lower content of Al+H species in the reference eroded samples than in the native or reclaimed soil indicates not only differences in the content of these chemical species but also differences in the degree of chemical weathering. The studied native Oxisol that originated from sediments dating from the Tertiary Period (e.g., phyllite and siltstone) has high levels of Al+H, thus it is intensely weathered and leached.

The Al species extracted with calcium chloride solution (0.01 mol L⁻¹) form rather stable complexes with SOM by reacting primarily with carboxyl groups and to a lesser extent with phenolic hydroxyl groups. The amount of Al-OM complex formed is dependent on pH and Al³⁺ concentration in solution (Bloom 1981; Hargrove and Thomas 1982). In the reclaimed soil, the content of Al+H was lower than in the native soil, which

Table 14. Ion intensities for m/z assigned to sterols and steroids in samples obtained from the 0–5 cm depth of native and reclaimed phases relative to a reference eroded Oxisol.

m/z	Identity	Ion intensity (counts mg^{-1})		
		Native	Reclaimed	Reference eroded
370	Cholestine	65 669	46 357	34 912
386	Cholesterol	45 504	19 587	17 267
394	Stigmastene	62 113	14 832	5 475
396	Ergosterol	37 731	23 767	7 612
400	Campesterol	43 323	28 916	24 417
410	Stigmasterol	19 755	10 474	5454
412	Stigmasterol	20 940	15 723	13 667
414	β -Sitosterol	19 629	19 308	17 482
416	Dehydro- β -sitosterol	16 778	12 038	5 929
426	D:A Friedooleanan-3-one	10 921	14 414	6 928
430	α -Tocopherol	9 391	7 690	5 382
Total*		348 002	217 868	137 742

*t test (total): native vs reclaimed $p = 0.008$; native vs reference eroded $p = 0.002$; reclaimed vs reference eroded $p = 0.0006$.

is also in agreement with the fact that after mechanically removing the top 8.6 m, the experimental plots were established on saprolite, a less weathered regolith present in the original native Oxisol (Kitamura et al. 2008; Taboada-Castro et al. 2009). Complementary information also shows that the amount of extractable Fe and Al influences the stabilization of soil C and its availability to soil microorganisms in non-volcanic and volcanic ash derived soils (Monreal et al. 1981; Parfitt and Parshotam 2002; Matus et al. 2014). Thus, our data suggest that most SOM may be found as organo-mineral complexes in the clay fraction, where Fe_2O_3 , Al oxides (i.e., gibbsite), and kaolinite predominate (Guilherme and Anderson 1998). The surface functional groups of inorganic and organic matter species in Oxisols help form strong organo-mineral complexes and in the adsorption of ions and heavy metals (Sposito 1984; Naidu et al. 1994), especially in the clay fraction than in the sand fraction (Chimchart et al. 2013). Future research is warranted on the organo-mineral complexes in the clay fraction of the Oxisol to examine the influence of pedogenesis and the soil reclamation practice on the type of chemical compounds and distribution of SOM at the nano- and micro-scales. To present, the temporal and spatial organization in architectural units and mechanisms of interactions of natural polymers of humic substances and their coverage of soil mineral surfaces are, to a large extent, still unclear (Dümig et al. 2012).

Table 15. Ion intensities for m/z assigned to esters of suberin in samples obtained from the 0–5 cm of native and reclaimed phases relative to a reference eroded Oxisol.

m/z	Ion intensity (counts mg^{-1})		
	Native	Reclaimed	Reference eroded
432	9 645	6 663	3 594
446	6 860	5 869	3 263
460	3 346	3 296	1 289
474	1 832	1 744	1 320
488	1 593	1 275	626
Total*	23 276	18 847	10 092

*t test (total): native vs reclaimed $p = 0.09$; native vs reference eroded $p = 0.03$; reclaimed vs reference eroded $p = 0.014$.

In addition, our results showed that thermally stable lipids, alkylaromatics, and N-heterocyclics volatilized at $>450^\circ\text{C}$ from the Oxisol samples, results that parallel the thermal stability shown by the same chemical classes of compounds observed in old SOM (i.e., 450–1200 years) residing in the clay and nano-size fractions of a thin Black Chernozem, and microaggregates $<50\ \mu\text{m}$ of a Gleysol of Canada (Monreal et al. 1997, 2010). From our data, we hypothesize that thermostable SOM classes (i.e., alkylaromatics, lipids, phenols+lignin monomers) in the Oxisol are associated with Fe, Al, and Si mineral species. Noteworthy, our findings on thermostable SOM are consistent with the hypothesis that alkylaromatics conform the central structural unit (i.e., backbone) of soil humic substances, to which other classes of compounds, such as lipids and phenols, are bound by covalent bonding during the biotic synthesis of soil humic substances via polyketides (Schnitzer and Monreal 2011). As determined by Py-FIMS, the native Oxisol presented about 100 times higher total molecular IIs than a Dark Brown Chernozem developed under native grassland, even though both soils have similar C content but with different pedogenetic histories (Schulten et al. 1995).

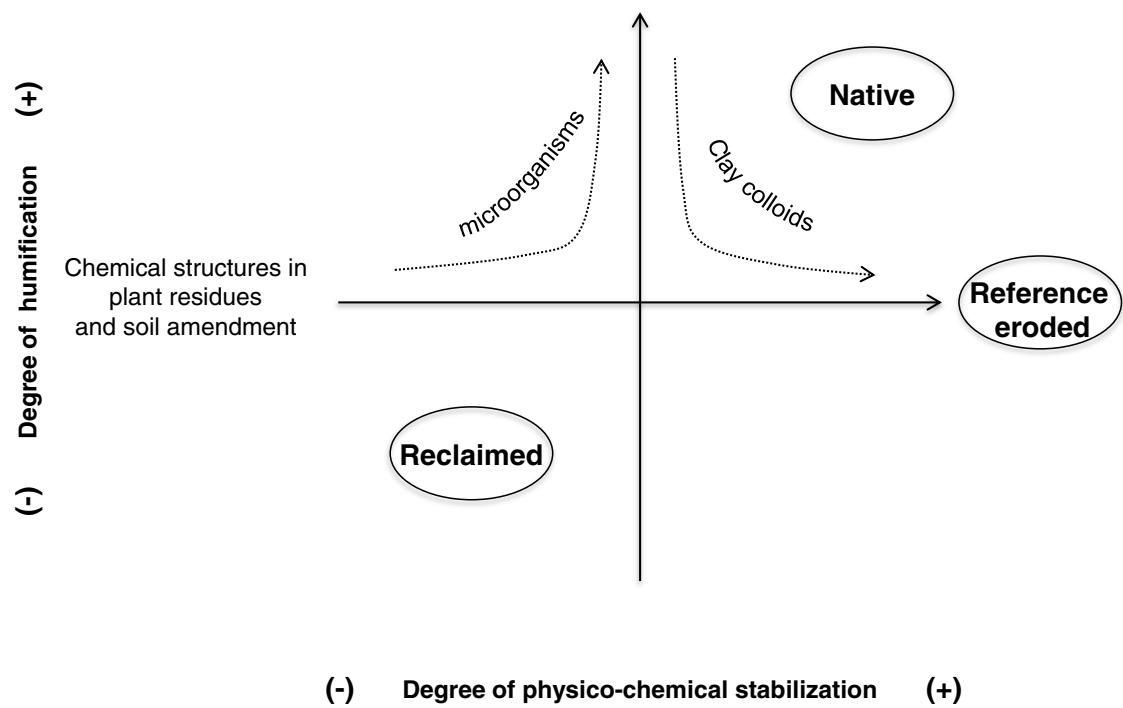
Figure 3 represents a simple model system that integrates data obtained from the elemental analysis, thermograms, and mass spectra during the chemical characterization of SOM by Py-FIMS. In Fig. 3, the x-axis represents the degree of physicochemical stabilization of SOM to colloidal surfaces of Fe-, Al-, and Si-containing minerals, and the y-axis represents the degree of humification of plant residues and dead microorganisms by active soil organisms. The curved dashed lines represent continuum domains that link biotic and abiotic processes in time and space. Figure 3 shows that SOM in the 0–5 cm depth of the reference eroded soil is found at the extreme of the x-axis, this is, being largely stabilized

Table 16. Summary of total ion intensities for *m/z* assigned to 13 chemical classes of compounds in the 0–5 cm depth of native and reclaimed phases relative to a reference eroded Oxisol.

Chemical class	Total ion intensity					
	Native		Reclaimed		Reference eroded	
	(counts mg ⁻¹)	(%)	(counts mg ⁻¹)	(%)	(counts mg ⁻¹)	(%)
Carbohydrates	1 441 288	3.3	1 621 471	3.7	806 179	1.8
Amino acids	643 381	1.5	747 673	1.7	407 780	0.9
Lignin monomers*	2 495 064	5.7	2 431 866	5.6	1 617 600	3.7
Lignin dimers	1 495 558	3.4	1 287 183	2.9	828 429	1.9
<i>n</i> -Alkylbenzenes	2 590 513	5.9	2 273 764	5.2	1 544 064	3.5
Flavonoids	1 082 467	2.5	977 447	2.2	624 883	1.4
<i>n</i> -Diols	2 062 558	4.7	1 749 394	4.0	1 200 472	2.7
Lipids†	11 140 331	25.5	9 131 714	20.9	5 892 989	13.5
N-Heterocyclics	8 156 450	18.7	7 860 123	18.0	4 605 390	10.5
Nitrile and other N-compounds	607 470	1.4	632 379	1.4	347 938	0.8
Alkyl radicals	522 856	1.2	387 345	0.9	158 120	0.4
Sterols and steroids	348 002	0.8	217 868	0.5	137 742	0.3
Esters of suberin	23 276	0.1	18 847	0.0	10 092	0.0
Total assigned‡	32 609 212	74.6	29 337 072	67.1	18 181 078	41.6
THI (15–900 <i>m/z</i>)	43 725 787	100	37 249 467	100	22 278 894	100
Volatile matter (%)		11		7		5

*Phenols + lignin monomers.
†Lipids = fatty acids + alkanes.
‡t test (total): native vs reclaimed *p* = 0.06; native vs reference eroded *p* = 0.01; reclaimed vs reference eroded *p* = 0.007.

Fig. 3. The degree of humification and physiochemical stabilization of soil organic matter in the 0–5 cm depth of the native, reclaimed, and reference eroded Oxisol.



by physicochemical reactions to inorganic minerals. The SOM in the reference eroded soil reflects mostly the presence of OM present in the saprolite before the removal of the top 8.6 m of soil material, as this reference soil has no C inputs such as plant or other organic residues. In addition, microbial humification processes would be negligible during the first 8 years of the experiment. Thus, SOM in the reference eroded soil is likely associated with old SOM leached over thousands of years from the A horizon, and less likely associated with rhizodeposition from native species or biotic humification, as indicated by the soil C/N ratio, and the small amount of microbial biomass indicated by the low abundance of ergosterol (m/z 396) (Table 14), an indicator of soil fungi (Montgomery et al. 2000), and esters of suberin, indicators of root polymer components (Table 15). In the native Oxisol, most SOM in the A horizon appears to be highly humified by microbial processing but also strongly bound to inorganic surfaces during pedogenesis, as indicated by C/N ratios and the thermal stability of SOM. Interestingly, the stable and possibly old SOM appears to be associated with structures of alkylaromatics, phenols, and lignin monomers and dimers, with contribution of *N*-heterocyclics, as indicated by Py-FIMS. In comparison, the SOM in the reclamation treatment represents, to a large extent, the effects of fresh organic residues returned by trees and grasses, roots, plus those in the sewage sludge. This SOM appears with relatively lower degree of microbial humification and physical stabilization than the SOM found in the native Oxisol, as indicated by the C/N ratio, the thermal evolution of volatilized chemical compounds, and the existing slow weathering regime. The abundance of thermolabile pools of carbohydrates, amino acids, and sterols contributed significantly to the SOM in the reclaimed soil. The interpretation of the main biotic and abiotic processes depicted in Fig. 3 shows the main influences of pedogenesis and soil reclamation on SOM content and chemical quality. These results show that the relative contributions of humification and abiotic stabilization processes on the chemical structures of SOM in the three Oxisol treatments.

Conclusions

Data from the elemental and Py-FIMS analysis show that relative to the reference eroded soil samples, total organic C and N contents in the top 5 cm of soil were highest in the native soil, followed by the reclaimed soil samples. The SOM in the surface layer of the reference eroded soil was mostly bound to inorganic colloids, with little influence of soil microorganisms. In the native treatment, SOM appeared to be highly humified and strongly bound to inorganic minerals, reflecting the long-term effect of biotic and abiotic pedogenetic processes. In the reclaimed soil, the chemistry of SOM reflects C and N inputs derived from fresh plant residues and sewage sludge, and reflects a low degree of

humification and physicochemical stabilization. Humified and thermally stable SOM involved mostly alkylaromatics, lipids, phenols+lignin monomers, lignin dimers, and *N*-heterocyclics. Conversely, thermolabile pools of SOM involved mostly carbohydrates, amino acids, and sterols, chemical classes that predominate the reclaimed Oxisol. Relative to the reference eroded and reclaimed soil samples, the native Oxisol presented a higher abundance of lignin dimers, *n*-alkylbenzenes, flavonoids, *n*-diols, *N*-heterocyclics, nitriles, alkyl radicals, and sterols plus steroids.

Acknowledgements

We thank the financial contributions made to this project by Universidade Estadual Paulista, the Coordenação de Aperfeiçoamento de Pessoal de Nível Superior (CAPES), Brazil, and Agriculture and Agri-Food Canada. The analyses of soil samples by Py-FIMS were conducted by P. Leinweber and Kai-Uwe Eckhardt of Rostock University.

References

- Alves, M.C., and Suzuki, L.G.A.S. 2007. Densidade do solo e infiltração de água como indicadores da qualidade física de um latossolo Vermelho Distrófico em recuperação. *Rev. Bras. Ciênc. Solo*. **31**: 617–625.
- Bloom, R.P. 1981. Metal-organic matter interactions in soil. *In* Chemistry in the soil environment. ASA Spec. Publ. 40. Edited by R.A. Dowdy. American Society of Agronomy, Madison, WI. pp. 129–150.
- Bonini, C.S.B., Dias, R.S., Alves, M.C., Abreu, C.A., Vázquez, E.V., and Paz-Ferreiro, J. 2015. Micronutrient content of a revegetated saprolite exposed by excavation of an Oxisol. *Commun. Soil Sci. Plant Anal.* **46**: 283–295. doi:10.1080/00103624.2014.989045.
- Chenu, C., and Plante, A.F. 2006. Clay-sized organo-mineral complexes in a cultivation chronosequence: revisiting the concept of the primary organo-mineral complex. *Eur. J. Soil Sci.* **57**: 596–607.
- Chimchart, B., Kheoruenromne, I., Suddhiprakarn, A., and Sparks, D.L. 2013. Role of organic matter on charge behaviour of oxisols and ultisols under tropical Savanna and tropical monsoon climates of Thailand. *Soil Sci.* **178**: 540–549. doi:10.1097/SS.0000000000000017.
- Dexter, A.R. 2004. Soil physical quality: part I. Theory, effects of soil texture, density, and organic matter, and effects on root growth. *Geoderma*. **120**: 201–214. doi:10.1016/j.geoderma.2003.09.004.
- Dümig, A., Werner, H., Stephens, W.M., and Kögel-Knabener, I. 2012. Clay fractions from a soil chronosequence after glacier retreat reveal the initial evolution of organo-mineral associations. *Geochim. Cosmochim. Acta*. **85**: 1–18.
- Empresa Brasileira de Pesquisa Agropecuária – EMBRAPA. 1997. Manual de métodos de análise de solo, 2nd ed. Centro Nacional de Pesquisa de Solos, Rio de Janeiro, Brasil. 212 p.
- Empresa Brasileira de Pesquisa Agropecuária – EMBRAPA. 2013. Sistema brasileiro de classificação de solos, 3rd ed. Rev. Ampl., Brasília, Brasil. 353 p.
- Fearnside, P.M. 1993. Deforestation in Brazilian Amazonia: the effect of population and land tenure. *Ambio*. **22**: 537–545.
- Feigl, B.J., Melillo, J., and Cerri, C.C. 1995. Changes in the origin and quality of soil organic matter after pasture introduction

- in Rondônia (Brazil). *Plant Soil*. **175**: 21–29. doi:[10.1007/BF02413007](https://doi.org/10.1007/BF02413007).
- Ferreira, C.A., Silva, A.C., Torrado, P.V., and Rocha, W.W. 2010. Genesis and classification of Oxisols in a highland toposequence of the upper Jequitinhonha Valley (MG). *Rev. Bras. Ciênc. Solo*. **34**: 195–209.
- Ferreira, D.F. 2008. Sisvar: versão 4.2. Um programa para análises e ensino de estatística. *Revista Symp*. **6**: 36–41.
- Guilherme, L.R., and Anderson, S.J. 1998. Copper sorption kinetics and sorption hysteresis in two oxide-rich soils (Oxisols). Effect of phosphate pretreatment. Chap. 9. In *Adsorption of metals by geomedial. Variables, mechanisms and model applications*. Edited by E.A. Jenne. Academic Press, San Diego, CA. pp. 210–229.
- Hargrove, W.L., and Thomas, G.W. 1982. Conditional formation constants for aluminum-organic matter complexes. *Can. J. Soil Sci.* **62**: 571–575. doi:[10.4141/cjss82-064](https://doi.org/10.4141/cjss82-064).
- Hempfling, R., and Schulten, H.-R. 1990. Chemical characterization of organic matter in forest soils by Curie-point pyrolysis-field ionization mass spectrometry. *Org. Geochem.* **15**: 131–145. doi:[10.1016/0146-6380\(90\)90078-E](https://doi.org/10.1016/0146-6380(90)90078-E).
- Hernández, R.M., and López, D. 2002. Microbial biomass, mineral nitrogen y carbon content in savanna soil aggregates under conventional and no-tillage. *Soil Biol. Biochem.* **34**: 1563–1570.
- Isaac, M.E., Gordon, A.M., Thevathasan, N., Oppong, S.K., and Quashie-Sam, J. 2005. Temporal changes in soil carbon and nitrogen in West African multistrata agroforestry systems: a chronosequence of pools and fluxes. *Agrofor. Syst.* **65**: 23–31. doi:[10.1007/s10457-004-4187-6](https://doi.org/10.1007/s10457-004-4187-6).
- Johnson, M.J., Lee, K.Y., and Scow, K.M. 2003. DNA fingerprinting reveals links among agricultural crops, soil properties, and the composition of soil microbial communities. *Geoderma*. **114**: 279–303. doi:[10.1016/S0016-7061\(03\)00045-4](https://doi.org/10.1016/S0016-7061(03)00045-4).
- Kitamura, A., Alves, M.C., Suzuki, L.G.A.S., and Gonzalez, A.P. 2008. Recuperação de um solo degradado com a aplicação de adubos verdes e lodo de esgoto. *Rev. Bras. Ci. Solo*. **32**: 405–416. doi:[10.1590/S0100-06832008000100038](https://doi.org/10.1590/S0100-06832008000100038).
- Kögel, I., Hempfling, R., Zech, R., Hatcher, P.G., and Schulten, H.-R. 1988. Chemical composition of the organic matter in forest soils. I. Forest litter. *Soil Sci.* **146**: 126–136.
- Lannes, L.S., Bustamante, M.M.C., Edwards, P.J., and Venterink, H.O. 2012. Alien and endangered plants in the Brazilian Cerrado exhibit contrasting relationships with vegetation biomass and N: P stoichiometry. *New Phytol.* **196**: 816–823. doi:[10.1111/j.1469-8137.2012.04363.x](https://doi.org/10.1111/j.1469-8137.2012.04363.x).
- Lavelle, P., and Pashanasi, B. 1989. Soil macrofauna and land management in Peruvian Amazonia (Yurimaguas, Loreto). *Pedobiologia*. **33**: 283–291.
- Matus, F., Rumpel, C., Neculma, R., Panichini, M., and Mora, M.L. 2014. Soil carbon storage and stabilization in andic soils: a review. *Catena*. **120**: 102–110. doi:[10.1016/j.catena.2014.04.008](https://doi.org/10.1016/j.catena.2014.04.008).
- Monreal, C.M., Etchevers, J.D., Acosta, M., Hidalgo, C., Padilla, J., López, R.M., Jiménez, L., and Velázquez, A. 2005. A method for measuring above- and below-ground C stocks in hillside landscapes. *Can. J. Soil Sci.* **85**: 523–530. doi:[10.4141/S04-086](https://doi.org/10.4141/S04-086).
- Monreal, C.M., McGill, W.B., and Etchevers, J. 1981. Internal nitrogen cycling compared in surface samples of an Andept and a Mollisol. *Soil Biol. Biochem.* **13**: 451–454. doi:[10.1016/0038-0717\(81\)90033-X](https://doi.org/10.1016/0038-0717(81)90033-X).
- Monreal, C.M., and Schnitzer, M. 2013. The chemistry and biochemistry of organic components in the soil solutions of wheat rhizospheres. Vol. 121. *Advances in Agronomy*. Edited by D.L. Sparks. pp. 179–251.
- Monreal, C.M., and Schnitzer, M. 2015. Labile organic matter in soil solution: II. Separation and identification of metabolites from plant-microbial communication in soil solutions of wheat rhizospheres. In *Labile organic matter – compositions, function, and significance in soil and the environment*. Edited by Z. He and F. Wu. Soil Science Society of America, Madison, WI. doi:[10.2136/sssaspecpub62.2014.0074](https://doi.org/10.2136/sssaspecpub62.2014.0074).
- Monreal, C.M., Schulten, H.-R., and Kodama, H. 1997. Age, turnover and molecular diversity of soil organic matter in aggregates of a Gleysol. *Can. J. Soil Sci.* **77**: 379–388. doi:[10.4141/S95-064](https://doi.org/10.4141/S95-064).
- Monreal, C.M., Sultan, Y., and Schnitzer, M. 2010. Soil organic matter in nano-scale structures of a cultivated Black Chernozem. *Geoderma*. **159**: 237–242. doi:[10.1016/j.geoderma.2010.07.017](https://doi.org/10.1016/j.geoderma.2010.07.017).
- Monreal, C.M., Zentner, R.P., and Robertson, J.A. 1995. The influence of management on soil loss and yield of wheat in Chernozemic and Luvisolic soils. *Can. J. Soil Sci.* **75**: 567–574. doi:[10.4141/cjss95-080](https://doi.org/10.4141/cjss95-080).
- Montgomery, H., Monreal, C.M., Young, J.C., and Seifert, K. 2000. Determination of soil fungal biomass from soil ergosterol analyses. *Soil Biol. Biochem.* **32**: 1207–1217. doi:[10.1016/S0038-0717\(00\)00037-7](https://doi.org/10.1016/S0038-0717(00)00037-7).
- Moreira, C.S., Casagrande, J.S., Ferracciú, L.R., de Camargo, O.A., and Berton, R.S. 2008. Niquel adsorption in two Oxisols and an Alfisol as affected by pH, nature of electrolyte, and ionic strength of soil solution. *J. Soils Sed.* **8**: 442–451. doi:[10.1007/s11368-008-0048-7](https://doi.org/10.1007/s11368-008-0048-7).
- Naidu, R., Bolan, N.S., Kookana, R.S., and Tiller, K.G. 1994. Ionic strength and pH effects on the sorption of cadmium and the surface charge of soils. *Eur. J. Soil Sci.* **45**: 419–429. doi:[10.1111/j.1365-2389.1994.tb00527.x](https://doi.org/10.1111/j.1365-2389.1994.tb00527.x).
- Parfitt, R.L., and Parshotam, A. 2002. Carbon turnover in two soils with contrasting mineralogy under long-term maize and pasture. *Aust. J. Soil Res.* **40**: 127–136. doi:[10.1071/SR00105](https://doi.org/10.1071/SR00105).
- Paz-Ferreiro, J., and Alves, M.C. 2012. Revegetation and soil management effects on chemical properties of a saprolite resulting from deep soil removal. *Comm. Soil Sci. Plant Anal.* **43**: 387–398. doi:[10.1080/00103624.2012.641796](https://doi.org/10.1080/00103624.2012.641796).
- Schnitzer, M., and Kodama, H. 1977. Reactions of minerals with soil humic substances. In *Minerals and their roles in the soil environment*. Edited by J.B. Dixon and S.B. Weeds. Soil Science Society of America, Madison, WI. p. 741.
- Schnitzer, M., and Monreal, C.M. 2011. Quo vadis soil organic matter research? A biological link to the chemistry of humification. *Adv. Agron.* **113**: 139–213.
- Schnitzer, M., and Schulten, H.-R. 1992. The analysis of soil organic matter by pyrolysis-field ionization mass spectrometry. *Soil Sci. Soc. Am. J.* **56**: 1811–1817. doi:[10.2136/sssaj1992.03615995005600060027x](https://doi.org/10.2136/sssaj1992.03615995005600060027x).
- Schulten, H.-R. 1984. Relevance of analytical pyrolysis studies to biomass conversion. *J. Anal. Appl. Pyrol.* **12**: 149–187. doi:[10.1016/0165-2370\(87\)85063-5](https://doi.org/10.1016/0165-2370(87)85063-5).
- Schulten, H.-R., Monreal, C.M., and Schnitzer, M. 1995. Effect of long-term cultivation on the chemical structure of soil organic matter. *Naturwissenschaften*. **82**: 42–44.
- Sorge, C., Schnitzer, M., and Schulten, H.-R. 1993. In-source pyrolysis-field ionization mass spectrometry and Curie-point pyrolysis-gas chromatography/mass spectrometry of amino acids in humic substances and soils. *Biol. Fertil. Soil.* **16**: 100–110. doi:[10.1007/BF00369410](https://doi.org/10.1007/BF00369410).
- Sposito, G. 1984. *The surface chemistry of soils*. Oxford University Press, New York.
- Taboada-Castro, M.M., Alves, M.C., Nascimento, V., and Taboada-Castro, M.T. 2009. Revegetation on a removed topsoil: effect on aggregate stability. *Comm. Soil Sci. Plant Anal.* **40**: 771–786. doi:[10.1080/00103620802686916](https://doi.org/10.1080/00103620802686916).

- Tyurin, I.V. 1953. Methods of analysis for the comparative study of soil humus composition. *Chem. Abstr.* **47**: 5597.
- Universidad de Huelva – UH. 2011. Servicios centrales de investigación. (S.l.:s.n., 200. Available from http://www.uhu.es/scid/uni_rayosx.html [accessed 30 January 2011].
- van Raij, B., Andrade, J.C., Cantarella, H., and Quaggio, J.A. 2001. Análise química para avaliação da fertilidade de solos tropicais. IAC, Campinas, Brasil. 285 p.
- van Veen, J.A., and Paul, E.A. 1981. Organic C dynamics in grassland soils. 1: background information and computer simulations. *Can. J. Soil Sci.* **61**: 185–201. doi:[10.4141/cjss81-024](https://doi.org/10.4141/cjss81-024).
- Wendling, B., Jucksch, I., de Sá Mendoça, E., de Almeida, R.F., Martins, C.E., and da Silva Domingues, L.A. 2014. Simulation of use and management effects on the soil organic matter pools of the Atlantic Forest biome, Brazil. *Biosci. J. Uberl.* **30**: 1278–1290.
- Zinn, Y.L., Lal, R., and Resck, D.V.S. 2005. Changes in soil organic carbon stocks under agriculture in Brazil. *Soil Tillage Res.* **84**: 28–40. doi:[10.1016/j.still.2004.08.007](https://doi.org/10.1016/j.still.2004.08.007).